

SCOOTER: A Human Evaluation Framework for Unrestricted Adversarial Examples

Dren Fazlja^{1*}, Monty-Maximilian Zühlke¹, Johanna Schrader^{1,4}, Arkadij Orlov²,
 Clara Stein¹, Iyiola E. Olatunji³, Daniel Kudenko¹

¹L3S Research Center, Leibniz University Hannover, Appelstr. 4, 30167, Germany.

²E.ON Grid Solutions, E.ON, Normannenweg 9, Hamburg, 20537, Hamburg, Germany.

³University of Luxembourg, Esch-sur-Alzette, L-4365, Luxembourg.

⁴CAIMed – Lower Saxony Center for AI & Causal Methods in Medicine, Appelstr. 9a, Hannover, 30167, Lower Saxony, Germany.

*Corresponding author(s). E-mail(s): dren.fazlja@L3S.de;

Contributing authors: zuehlke@L3S.de; schrader@L3S.de; arkadij.orlov@eon.com;
clara.stein@L3S.de; emmanuel.olatunji@uni.lu; kudenko@L3S.de;

Abstract

Unrestricted adversarial attacks aim to fool computer vision models without being constrained by ℓ_p -norm bounds to remain imperceptible to humans, for example, by changing an object’s color. This allows attackers to circumvent traditional, norm-bounded defense strategies such as adversarial training or certified defense strategies. However, due to their unrestricted nature, there are also no guarantees of norm-based imperceptibility, necessitating human evaluations to verify just how authentic these adversarial examples look. While some related work assesses this vital quality of adversarial attacks, none provide statistically significant insights. This issue necessitates a unified framework that supports and streamlines such an assessment for evaluating and comparing unrestricted attacks. To close this gap, we introduce SCOOTER – an open-source, statistically powered framework for evaluating unrestricted adversarial examples. Our contributions are: *(i)* best-practice guidelines for crowd-study power, compensation, and Likert equivalence bounds to measure imperceptibility; *(ii)* the first large-scale human vs. model comparison across 346 human participants showing that three color-space attacks and three diffusion-based attacks fail to produce imperceptible images. Furthermore, we found that GPT-4o can serve as a preliminary test for imperceptibility, but it only consistently detects adversarial examples for four out of six tested attacks; *(iii)* open-source software tools, including a browser-based task template to collect annotations and analysis scripts in Python and R; *(iv)* an ImageNet-derived benchmark dataset containing 3K real images, 7K adversarial examples, and over 34K human ratings. Our findings demonstrate that automated vision systems do not align with human perception, reinforcing the need for a ground-truth SCOOTER benchmark.

Keywords: Unrestricted Adversarial Examples, Subjective Image Quality Assessment, Adversarial Machine Learning, Computer Vision, Online Data Collection, Human Perception

1 Introduction

With an ever-increasing reliance on computer vision (CV) models in the real world, assessing and ensuring the safety and robustness of these systems becomes increasingly relevant, especially in critical domains such as autonomous driving or healthcare. However, malicious entities can mislead CV models by deliberately adding noise that is imperceptible to humans (Szegedy et al., 2014). Such deceptively modified images, known as *adversarial examples* (AEs), appear benign to the human eye, yet can trigger misclassifications in the model. One way to ensure the imperceptibility of this adversarial noise is *restricting* perturbations via ℓ_p -norms, but these attacks can often be mitigated through image pre-processing (Dziugaite, Ghahramani, & Roy, 2016), certified robust defense strategies (Li, Xie, & Li, 2023), and, most notably, adversarial training (Madry, Makelov, Schmidt, Tsipras, & Vladu, 2018). Hence, *unrestricted* AEs have garnered increasing interest. These attacks alter images through modifications humans easily overlook, for example, by manipulating semantic information. Shamsabadi, Sanchez-Matilla, and Cavallaro (2020) perform color changes exclusively to non-sensitive areas (e.g., unrelated object details) that look natural across a wide range of colors to the human eye. However, because of their unrestricted nature, there are no norm-based imperceptibility guarantees, demanding human evaluations to verify the imperceptibility of these adversarial examples. Although few works (Bhattad, Chong, Liang, Li, & Forsyth, 2020; Dai, Liang, & Xiao, 2025; Liu, Zhang, & Zhang, 2023; Qiu et al., 2020; Sharif, Bhagavatula, Bauer, & Reiter, 2019; Song, Shu, Kushman, & Ermon, 2018) employ human evaluation experiments to support their claims, none offer statistically significant insights. Developing a statistically sound human evaluation framework is challenging because it requires sufficiently large samples of reliable and unbiased human data. Additionally, researchers have to apply appropriate statistical analyses to subjective judgments. While some guidelines exist (e.g., (Aguinis, Villamor, & Ramani, 2021)), incorporating and adjusting them to this domain is tedious and challenging. Hence, it is crucial to provide the research community with a statistically significant human evaluation protocol covering

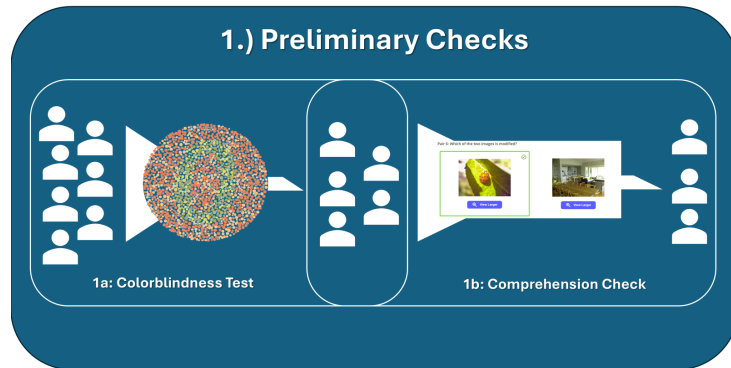
best practices of study design, which is the goal of this work.

To facilitate research into unrestricted adversarial examples, we propose SCOOTER (Systemizing Confusion Over Observations To Evaluate Realness) – a human evaluation framework for examining the quality of unrestricted adversarial images (i.e., the imperceptibility of modifications). Drawing inspiration from existing tools (Otani et al., 2023) and following established study design recommendations (Aguinis et al., 2021), SCOOTER enables researchers to make statistically significant claims about the imperceptibility of image-based attacks. In Fig. 1, we provide an overview of our proposed end-to-end process to assess unrestricted AEs. Our contributions in this work are as follows: (i) we design a carefully crafted **study protocol** that guides researchers in **every step** of performing online studies; (ii) we use our protocol to conduct a **benchmarking study** which highlights the pitfalls of previous work regarding attack imperceptibility; (iii) we develop a **ready-to-use web application** with a modular design allowing researchers to integrate their AEs easily; (iv) we create an **image database** that includes all generated AEs based on a subset of unmodified ImageNet (Russakovsky et al., 2015) images (**ImageNet S-R50-N**) for further analysis. We have released the source code for reproducing our experiments at <https://github.com/DrenFazlja/SCOOTER>. The associated image dataset is publicly available on Zenodo via the following DOI: <https://doi.org/10.5281/zenodo.15771501>.

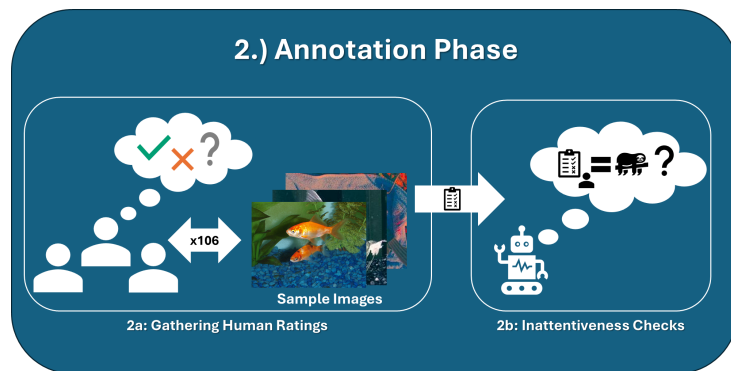
2 Related Work

2.1 Image-Based Adversarial Examples

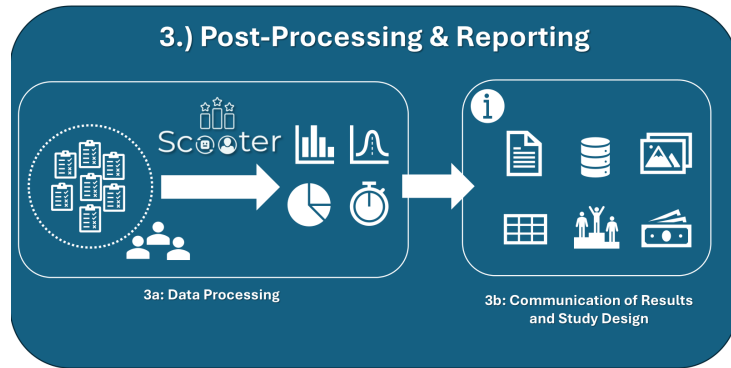
Restricted Attacks. Traditionally, image-based adversarial attacks cause models to misclassify inputs by slightly altering pixels. Concretely, attackers restrict the maximum allowed perturbation via an ℓ_p -norm (e.g., (Carlini & Wagner, 2017; Goodfellow, Shlens, & Szegedy, 2015; Modas, Moosavi-Dezfooli, & Frossard, 2019)) to avoid human detection. For instance, ℓ_∞ -based restrictions (Goodfellow et al., 2015) limit the maximum change per pixel to keep the total



(a) **Phase 1:** Preliminary Checks



(b) **Phase 2:** Annotation Phase



(c) **Phase 3:** Statistical Analysis & Reporting

Fig. 1 The SCOOTER framework. Recruited participants first have to pass two preliminary checks (Fig. 1a): (i) a colorblindness test, as most unrestricted attacks adjust the images' colors, and (ii) a comprehension check to verify that they understand the task. The remaining participants will then be forwarded to the main part of the study (Fig. 1b), where they annotate images. Using appropriate checks, researchers can filter out inattentive participants, and after collecting sufficient annotations, gather key results and study statistics (Fig. 1c). Finally, researchers can (i) use templates to report and compare their attack's imperceptibility, (ii) publish their generated data, and (iii) compensate participants for their efforts following our guidelines.

change limited and the resulting images close to the data manifold. However, these norm-based *restricted* attacks come with multiple disadvantages. For one, image pre-processing methods can smooth out malicious small-scale changes made by the adversary (Dziugaite et al., 2016; Xu, Evans, & Qi, 2018). Additionally, adversarial training (Madry et al., 2018) with the same norm can significantly mitigate a model’s susceptibility to adversarial noise. Moreover, methods exist to certify robustness against these attacks (Li et al., 2023). While restrictions via alternative perceptual metrics (e.g., (Sielmann & Stelldinger, 2023; Wong, Schmidt, & Kolter, 2019; Zhao, Liu, & Larsson, 2020)) are more promising than traditional approaches, their restricted nature limits effectiveness (Laidlaw, Singla, & Feizi, 2021). Additionally, recent work has shown that standard perceptual metrics do not necessarily align with human perception (Stein et al., 2023). For this reason, we focus on *unrestricted* adversarial attacks.

Unrestricted (Content-Based) Attacks.

Researchers have begun exploring unrestricted approaches as alternative methods to generate AEs. Instead of minuscule changes to pixels, attackers employ semantically coherent or *content-based* changes to an image. For instance, some regions in an image (e.g., a wall in the background) look natural in various colors. In contrast, the number of plausible colors for more sensitive regions (e.g., a person or the sky) is very restricted. Some attacks (e.g., (Shamsabadi, Sanchez-Matilla, & Cavallaro, 2020; Yuan, Zhang, Gao, Cheng, & Song, 2022)) consider this information to recolor suitable areas of an image to create benign-looking AEs. Attackers can also adjust the texture of objects within an image (Bhattad et al., 2020) or adjust key semantic features of the image (e.g., hair color of portrait images (Qiu et al., 2020)). Other works propose altering an image’s latent representation as any minor change to the lower-dimensional latent coincides with semantically higher-level transformations. As a result, decoding the perturbed latent representation leads to unrestricted AEs (X. Chen, Gao, Zhao, Ye, & Xu, 2023; Z. Chen et al., 2023; Xue, Araujo, Hu, & Chen, 2023). These more modern attacks and other adjacent strategies (Kang, Song, & Li, 2023; Zhang, Zhang, & Wischik, 2024) represent *diffusion-based* attacks, as they rely on the image

generation capabilities of diffusion models (Ho, Jain, & Abbeel, 2020; Sohl-Dickstein, Weiss, Maheshwaranathan, & Ganguli, 2015). Another line of work generates AEs from scratch instead of modifying existing images (Song et al., 2018). However, our study focuses on assessing the quality of manipulated images by evaluating their discrepancy from a reference data distribution.

Human Quality Assessment of Unrestricted AEs. A core characteristic of image-based AEs is their imperceptible nature: while they need to fool ML models, they must still appear as natural and unmodified as possible to humans. In our review of the literature on unrestricted AEs we found two recurring gaps: many papers neglect image quality evaluation altogether (Hosseini & Poovendran, 2018; Joshi, Mukherjee, Sarkar, & Hegde, 2019; Kang et al., 2023; Xiang, Liu, Guo, Gan, & Liao, 2022), and many others rely only on automated metrics (X. Chen et al., 2023; Z. Chen et al., 2023; Na, Ji, & Kim, 2022; Shamsabadi, Sanchez-Matilla, & Cavallaro, 2020; Yang, Song, & Wu, 2021) that poorly predict human perception (Stein et al., 2023). Several studies do enlist human raters (Bhattad et al., 2020; Dai et al., 2025; Liu et al., 2023; Qiu et al., 2020; Sharif et al., 2019; Song et al., 2018; Zhang et al., 2024), and more recent work asks different perceptual questions, such as whether time-limited observers misclassify ℓ_p perturbations (Elsayed et al., 2018), whether spatially masked noise is noticed (Göpfert, Artelt, Wersing, & Hammer, 2020), or how latent-diffusion representations align with human similarity judgments (Linhardt, Morik, Bender, & Borras, 2024). However, none of these studies adequately measures the imperceptibility of unrestricted attacks. Moreover, they typically omit one or more key components of a reproducible online experiment, including transparent reporting of participant demographics, effect sizes, compensation and time commitment, a priori power analysis, prescreening filters, and attentiveness checks (see Fig. 1). We refer the reader to (Aguinis et al., 2021) for a survey of crowdsourcing pitfalls—all of which SCOOTER addresses (Sec. 3).

2.2 Relevant State-of-the-Art Protocols

The most similar work to ours is the evaluation protocol of (Otani et al., 2023), analyzing the quality of Text-To-Image generators. The authors provide researchers with well-designed domain-specific questions and user interfaces, recommendations for several design choices (e.g., requirements that participants need to fulfill), and templates for reporting human evaluation results. Unfortunately, their protocol does not sufficiently guide inexperienced researchers in the difficult aspects of experiment design, such as appropriate participant filters and statistically grounded analyses. Notably, there is a lack of methods to guarantee high-quality evaluation data. For instance, their protocol does not cover standard measures like attention and instruction manipulation checks. The authors also publicly state their eligibility requirements, which can lead to increased self-misrepresentation of participants (Aguinis et al., 2021; Bauer et al., 2020). Another adjacent publication (S. Zhou et al., 2019) provides a basic framework for collecting human image quality assessments. While the resulting protocols $HYPE_{time}$ and $HYPE_{\infty}$ are widely used in subjective image quality assessment tasks, they exhibit similar weaknesses to those in (Otani et al., 2023), such as the lack of appropriate participant filters. In contrast to prior work, and as visualized in Fig. 1, our objective is to support both experienced and inexperienced researchers by rigorously defining every detail of the study design, including transparent compensation policies, priming-free task descriptions and participant filters, and step-by-step instructions for a sound statistical evaluation. Furthermore, this work represents the realization of a prototype we introduced in an extended abstract (Fazlja et al., 2024).

3 The SCOOTER Pipeline in Three Phases

The SCOOTER framework (as visualized in Fig. 1) addresses several challenges of a representative human evaluation study design. As outlined by (Aguinis et al., 2021), these challenges, hereafter referred to as **C1** through **C10**, include inattentive participants (**C1**), self-misrepresentation (**C2**), self-selection bias (**C3**, i.e., humans who

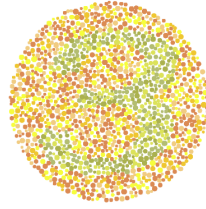
participate in online studies may not represent broader populations), high-attrition/drop-out rates (**C4**), inconsistent English language fluency (**C5**), non-naivete/priming of participants (**C6**), communication between participants (**C7**), vulnerability to web robots (**C8**), social desirability bias (**C9**, i.e., participants may feel inclined to choose socially accepted answers), and perceived researcher unfairness (**C10**). In this section, we outline how SCOOTER addresses these challenges. To evaluate the imperceptibility of unrestricted attacks, we propose conducting an **18-minute** online study using services like Prolific (Prolific, 2025) with a fair compensation base rate (e.g., £9 per hour as of Prolific’s 2025 guidelines). This estimated completion time stems from the data collected from our first three experiments ($n = 196$, see Sec. 4.1 for details; this addresses **C1**, **C4** by striking a fair balance between the number of collected annotations and the participants’ time investment), where the completion time remained consistent across all attacks. Prolific allows researchers to prescreen participants without publicly sharing eligibility requirements (**C2**, **C9**) while providing data of higher quality than other services (Douglas, Ewell, & Brauer, 2023). We use the built-in prescreeners to filter out colorblind workers and those who self-report as not fluent in English (**C2**, **C3**, **C5**). We further ensure workers’ capabilities by performing a short colorblindness and comprehension check (**C1**, **C2**, **C5**). We describe the instantiation of adjustable study parameters (e.g., the provided compensation) in Appendix B. Additionally, our appendix also includes text templates for posting Prolific jobs, which specifically avoid participant priming (see Appendix A.1; **C6**). In the following sections, we detail the three core phases of the SCOOTER pipeline: (1) preliminary participant checks to ensure data quality, (2) the main study phase focused on evaluating the imperceptibility of adversarial examples (AEs), and (3) statistical significance testing and reporting practices to support transparency and reproducibility.

3.1 Preliminary Checks

Here, we detail the preliminary checks that participants are required to complete before proceeding with the main task.

Colorblindness Test

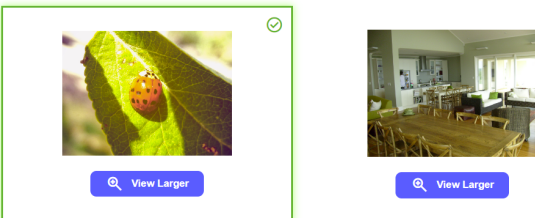
Please enter the digit you see in the image.



0 1 2 3 4 5 6 7 8 9 I don't see a digit

(a) The Colorblindness Check Interface

Pair 6: Which of the two images is modified?



(b) The Comprehension Check Interface

Image Annotation Task



Is this image real or modified?

Definitely Modified Probably Modified Unsure Probably Real Definitely Real

(c) The Main Study Interface

Fig. 2 The user interface for the two preliminary checks and the main study of SCOOTER.

Colorblindness Check. The most prominent attack vectors for unrestricted AEs are the colors of an image. As such, we expect colorblind annotators to overestimate the imperceptibility of

most attacks. Thus, participants must correctly classify five different Ishihara-like images (Ishihara, 1917) before accessing the study's central portion (see Figs. 1a and 2a; C1, C2). These

images can be found on Kaggle (Lyakhov, 2020) and emulate so-called Ishihara plates – diagnostic mainstays for color vision deficiency, whose administration is regarded as a fundamental competency in ophthalmology (Bron et al., 2024). We informed participants that misclassifying at least one image would disqualify them, though they would still be compensated for their time (**C1**, **C4**, **C10**).

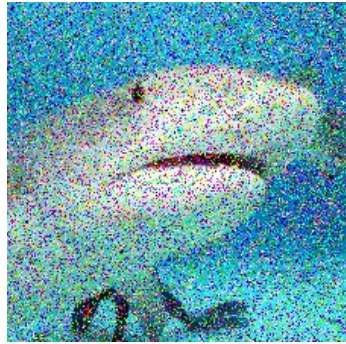
Comprehension Check. After passing the colorblindness check, we provide participants with a brief explanation outlining common image modification strategies. Examples include image filters and the change of colors in a particular area of the image. After reading the explanation, the participant must pass a comprehension check (**C1**, **C2**). Our prescreening of non-fluent English speakers and this check adequately address concerns about inconsistent English fluency (**C5**), ensuring that participants have the necessary language skills to understand and complete the image rating task without additional language measures typically required in text-based studies. We then display six image pairs, each containing a random unmodified image and a random modified image (see Figs. 1a and 2b) to the participant.

To create the pairs, we selected 35 images from ImageNet-V2 (Recht, Roelofs, Schmidt, & Shankar, 2019) as our unmodified baseline, covering each of the 11 semantic ImageNet classes (Tsipras, Santurkar, Engstrom, Ilyas, & Madry, 2020). We manually created modified counterparts via the online image editor *Photo Filters* (Zygomatic, 2025). Modifications include inconsistent recoloring of images, adding prominent noise, and applying image filters. After filtering out overly difficult instances through our series of experiments (see Appendix C.3 for details), we are left with 23 unmodified and 86 modified images (**C7**, as participants who were filtered out may motivate others to avoid this study). We do not employ any attacks to create modified images, thereby avoiding method-specific biases. We informed participants that misclassifying two or more image pairs would result in disqualification, although they would still be compensated for their time (**C1**, **C4**, **C10**). To proceed to the main part of the study, participants must correctly identify the modified image in at least five out of the six pairs.

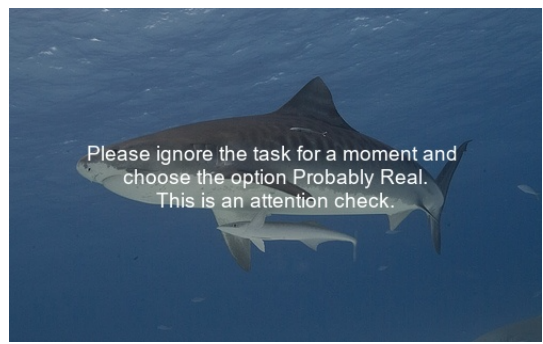
3.2 The Main Study

Here, we aim to analyze the imperceptibility of AEs generated to fool one specific model. As depicted in Fig. 1b, we evaluate generated AEs by asking participants to rate the degree of modification for 106 images. The number of images aligns with adjacent work (S. Zhou et al., 2019) and represents a sufficiently large set of images that can be annotated within a reasonable time. Contrary to previous works, we do not rely on a forced binary choice between “modified” and “unmodified”. Instead, we want participants to rate how confident they are about the degree of modification using a 5-point Likert scale (Likert, 1932) (see Fig. 2c). The input ranges from *Definitely Modified* (−2) to *Definitely Real* (+2). We believe that our rating scale provides more insight into the imperceptibility of unrestricted attacks than previously used forced-binary choice rating systems. Participants annotated 50 of 2,966 ImageNet S-R50-N images (see Sec. 4 and Appendix D for details about the dataset) and 50 modified instances produced by the respective attack. Because each assignment is independent and random, (i) participants may not see the same images, and (ii) they might not view the real and modified versions of the same image. Nevertheless, every participant rates both real and adversarial images, rendering this a *within-subject repeated-measures design*. Lastly, 6 attention check items were included to detect and filter out inattentive participants (see below).

Inattentiveness Checks in the Main Study. In line with existing guidelines (Aguinis et al., 2021; Ward & Meade, 2023), we use both *bogus items* (here: clearly modified images) and *instruction manipulation checks* (IMCs; i.e., we instruct participants to choose a pre-defined option) to check for inattentiveness (**C1**, **C8**). Concretely, bogus items are represented by three different level-5 severity instances of ImageNet-C (Hendrycks & Dietterich, 2019) (see Fig. 3a). In contrast, IMCs represent three different ImageNet samples containing pre-defined written annotator instructions (see Fig. 3b). Participants *fail* a bogus item if they rate it as > -1 , i.e., higher than “Probably Modified”. In contrast, they fail an IMC if they do not choose the pre-defined option. Participants are marked as *inattentive* if they fail at least two of the six attention check



(a) Bogus Item Example



(b) Instruction Manipulation Check

Fig. 3 Examples of attention check images used in SCOOTER. We assign each participant to three bogus items and three instruction manipulation checks.

items. To mitigate fatigue-related poor performance, we ensured that all 6 attention check items (3 of each category) were included within the first three-quarters of the total test images.

Based on our collected data, we also investigated additional metrics to detect inattentiveness. For instance, item-level metrics like Person-total correlation (Curran, 2016) are *not compatible* with SCOOTER, as they would require all participants to rate the same images. However, as we do not want participants to memorize and share study details (C7), we avoid limiting the SCOOTER main study to a small number of sample images. Furthermore, some potentially applicable metrics like the Mahalanobis-Distance (Mahalanobis, 2018), even-odd inconsistency (Jackson, 1976), and resampling strategies (Curran, 2016) did not provide conclusive results for our data. As such, drawing from the experiments in Sec. 4, researchers *may* also filter out inattentive participants via (i) the average time spent on an image, (ii) Long-String statistics (Johnson, 2005) (i.e., how often did a participant choose the same option in a row¹) and (iii) Intra-individual response variability (IRV) (Dunn, Heggestad, Shanock, & Theilgard, 2018). IRV is equivalent to the standard deviation of a participant’s real and modified ratings. Table 1 summarizes the different thresholds that should be used to filter out inattentive respondents instantly (“hard rules”). It also outlines additional recommendations to filter out participants based on the observed 99th percentile

¹Note: Keep in mind that participants can choose between five different options. E.g., *probably* modified and *definitely* modified count as two different options.

Metric	Thresholds
Hard Rules	
Failed colorblindness checks	≥ 1 of 5
Failed comprehension checks	≥ 2 of 6
Failed attention checks	≥ 2 of 6
Recommendations (99th Percentile)	
Average Time per Image	\leq 2.5 seconds
Max. Sequence Length	\geq 11
Mean Sequence Length	\geq 2.14
Median Sequence Length	\geq 2
IRV _{real}	$<$ 0.3871
IRV _{modified}	$>$ 1.8104

Table 1 Thresholds to filter out inattentive participants. Triggering any of the hard rules led to reduced compensation. Based on the empirical results from Secs. 4.1 and 4.2, we also recommend that future work filter out participants based on the values reported within the 99th percentile section.

of different statistics in future SCOOTER studies. However, as our original experiments did not utilize these additional filters, these *may* but do not *need* to be enforced. Appendix E outlines details and an ablation study to investigate more gradual inattentiveness filtering. Participants were informed about the existence of attention checks and the consequences of failing them before the study (C1, C4, C10).

3.3 Statistical Significance and Reporting

As visualized in Fig. 1c, researchers should report study details for reproducibility. For SCOOTER-based studies, this includes the core rating metrics

and the metrics revolving around the performed *equivalence test*. Additionally, we recommend that researchers report information surrounding the study itself. This includes the number of participants (including those who were filtered out), a demographic summary of eligible participants, the provided compensation, the average and median time commitment for the entire study, and the main study image annotation. Optionally, researchers can also report the median time of successful colorblindness and comprehension check tests. Note that SCOOTER calculates all of these metrics by default. Appendix A provides appropriate sample texts.

Core Metrics. Beyond the attack’s success rate (ASR) against the victim model (i.e., the ratio of successfully generated AEs), we are interested in the mean ratings of modified and real images, denoted by μ_{modified} and μ_{real} , respectively. The mean modified score, μ_{modified} , reflects the average rating of a modified image from a particular attack, ranging from -2 (*definitely modified*) to $+2$ (*definitely real*). A higher score suggests the modified images were perceived as "more real". Consequently, a high μ_{modified} corresponds to high imperceptibility. In terms of classification errors (positive class = "real"), a high μ_{modified} signals a high false positive rate. The real image score, μ_{real} , on the other hand, allows us to judge the imperceptibility of two attacks when they share similar modified scores — the larger the gap between μ_{modified} and μ_{real} , the less imperceptible the attack. When conducting studies, researchers should report additional information about the ratings (e.g., the observed standard deviation) to allow comparability.

Equivalence Testing. Most human studies test whether a given intervention (e.g., a reworked user interface) demonstrates a *significant effect* compared to a baseline (e.g., the current interface design). Following common recommendations, researchers fix a desired significance level α (e.g., $\alpha = 0.05$) and a statistical power target $1 - \beta$ (e.g., $1 - \beta = 0.95$) in advance. They then collect participant feedback (e.g., via Likert-scale ratings) and perform the appropriate statistical test to obtain the resulting p -value. In our running example, a higher mean rating for the newer design and $p < 0.05$ would indicate that there is a significant effect between the two interface

designs, i.e., there is statistically significant evidence that the new design is received better by the participants. In other words, researchers are mostly interested in checking whether an intervention leads to a significant *difference* compared to the baseline. However, in SCOOTER experiments, we have the exact opposite goal: We want to demonstrate that our intervention (the adversarial attack) leads to a *similar* outcome (perception of realness) when compared to our baseline (the original real images). One may be inclined to perform a test akin to the above running example and use the resulting p -value to judge the imperceptibility of an attack: if $p < 0.05$, then there is a significant difference between the perception of real and modified images; otherwise ($p \geq 0.05$) the images generated by the attack are indistinguishable from real images. However, in the latter case, we, in fact, *cannot* form any conclusion about the attack’s imperceptibility. As noted by Altman and Bland (1995) and outlined in Chapter 9 of (Lakens, 2022), *[the] absence of evidence is not evidence of absence* — we cannot simply assume that real and modified images are indistinguishable from one another because we could not prove significant differences between their ratings. To demonstrate an attack’s imperceptibility (i.e., its similarity to the real image baseline), we have to perform an *equivalence test* using the two-one-sided tests (TOST) procedure (Schuirmann, 1987). In TOST, we aim to prove that the observed metric (here: mean Likert-scale ratings) of the two groups (real and modified images) are similar enough according to a predefined range of scores. Concretely, the *Null Hypothesis* (H_{01} or H_{02}) states that the rating distributions for the real and modified images are not *practically equivalent*, i.e., $\Delta := \mu_{\text{real}} - \mu_{\text{modified}} < \Delta_L$ or $\Delta > \Delta_U$, whereas the *Alternative Hypothesis* (H_A) states that the ratings are *practically equivalent*, i.e., $\Delta_L \leq \Delta \leq \Delta_U$. Here, Δ_L and Δ_U define the range of rating score differences we still consider "practically equivalent." For instance, $\Delta_L = -0.2$ and $\Delta_U = +0.2$ means that we consider μ_{modified} and μ_{real} to be similar enough as long as neither image category (real or modified) deviates from the other by more than 0.2 rating points. Failing the lower-bound test (i.e., $\Delta < \Delta_L$) implies that modified images are rated higher than real images beyond

the acceptable margin, whereas failing the upper-bound test (i.e., $\Delta > \Delta_U$) implies that real images are rated higher than modified images beyond the margin. Both outcomes would imply that benign and adversarial distributions are not practically equivalent w.r.t the ± 0.2 thresholds.

How to Perform TOST for SCOOTER.

As done in (Judd, Westfall, & Kenny, 2012), researchers first have to fit a linear mixed-effects model on their data using packages like `lme4` (Bates, Mächler, Bolker, & Walker, 2015) to account for the random assignment of modified and real images to participants (i.e., each participant only annotates a randomly sampled subset of both image categories) before they can perform TOST. Based on the approach proposed in (Isager, 2019), researchers can then use the model’s corresponding fixed effect size and degrees of freedom to perform TOST. SCOOTER comes with adequate R code to perform said analysis with our empirically motivated equivalence bounds (see Sec. 4.1.4 for details). Researchers should report the resulting p -values for both the lower bound ($\Delta < \Delta_L$) and upper bound ($\Delta > \Delta_U$) hypothesis test and only reject the null hypothesis if *both* values are below the pre-defined significance threshold α .

4 Experiments

To demonstrate the functionality and importance of the SCOOTER framework, we assessed the quality of **three unrestricted, color-based attacks**, as the colors of an image are the most prominent attack vector (cf. Sec. 4.1). These three attacks (sorted by the complexity of their attack strategy) are SemanticAdv (short: SemAdv) (Hosseini & Poovendran, 2018), cAdv (Bhattad et al., 2020), and Natural Color Fool (short: NCF) (Yuan et al., 2022). Results from this initial trio provided the empirical basis for all subsequent design decisions, including the compensation rate (with a base rate of £9 per hour), expected task duration, target sample size, and the upper and lower equivalence bounds $\Delta_{U/L}$. We also incorporated participant feedback throughout the three experiments to improve the SCOOTER framework. As the resulting design differences are minor, we report all changes made between experiments in Appendix C (including changes to the UI and the compensation).

Building on this foundation, we conducted a second series of experiments to evaluate **diffusion-based unrestricted attacks**, using the same recruitment strategy, compensation, and power parameters as before (see Sec. 4.2 for details). These attacks are DiffAttack (DA) (Kang et al., 2023), AdvPP (Zhang et al., 2024), and ACA (Z. Chen et al., 2023). This extension allows us to investigate whether the imperceptibility gap we observed for color attacks persists when an attacker leverages modern generative models. Our working hypothesis remains simple: the more sophisticated the attack strategy, the more convincing its adversarial examples (AEs) will be. The remainder of this section introduces our new dataset and the computer vision (CV) model that the attacks aim to fool (the so-called *victim model*). Finally, we examine how closely the ratings produced by a state-of-the-art vision-language model (see Sec. 4.3) and those obtained through objective image-quality metrics (see Sec. 4.4) align with human judgments.

Victim Model. The choice of victim model is crucial for our study design. Because ResNet-50 (He, Zhang, Ren, & Sun, 2015) is widely used as a computer vision baseline model, especially in unrestricted attack literature, e.g., (Bhattad et al., 2020; Z. Chen et al., 2023; Hosseini & Poovendran, 2018; Kang et al., 2023; Shamsabadi, Oh, & Cavallaro, 2020; Shamsabadi, Sanchez-Matilla, & Cavallaro, 2020; Yuan et al., 2022; Zhang et al., 2024), we focus on this architecture. However, instead of the standard ResNet-50 model, which is vulnerable to classic, restricted attacks, we opted for the adversarially trained model from (Salman, Ilyas, Engstrom, Kapoor, & Madry, 2020), as it is the most robust version against norm-based attacks (Croce et al., 2021). This choice ensures that any adversarial example must introduce changes exceeding standard norm bounds, providing a more stringent test of imperceptibility. We will refer to our victim model as *ResNet-50-AT_{norm}*.

Dataset. Due to the greater susceptibility of models to high-resolution images, we opt to benchmark perturbed ImageNet-1k images (Russakovsky et al., 2015) as they are widely used in unrestricted attack literature (e.g., (Bhattad et al., 2020; Shamsabadi, Oh, & Cavallaro, 2020; Shamsabadi, Sanchez-Matilla, & Cavallaro, 2020;

Color-based Attacks (§4.1)

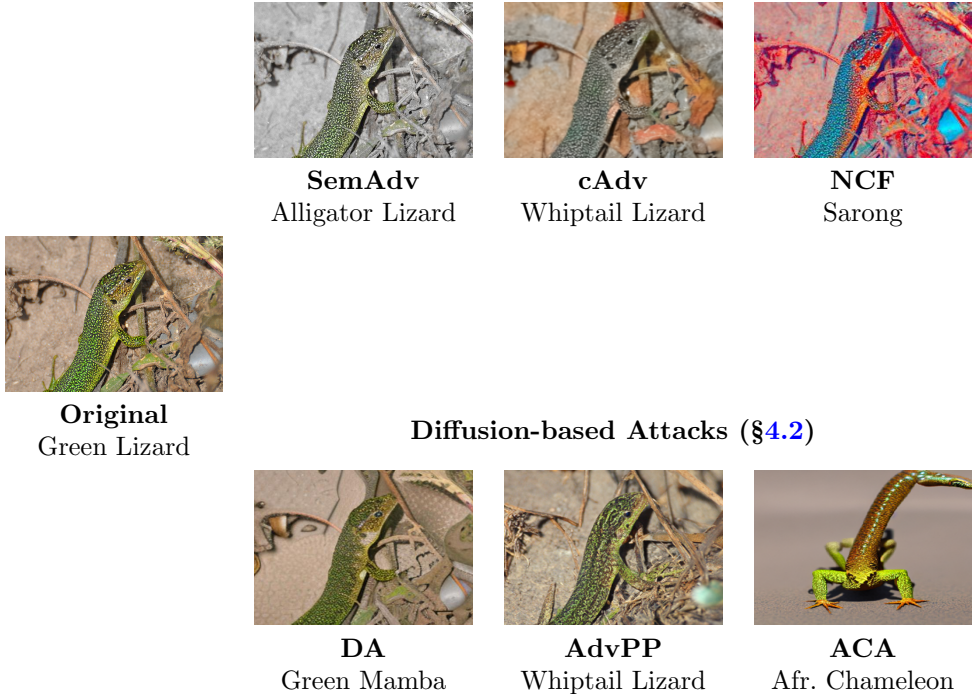


Fig. 4 An ImageNet S-R50-N image for which *all six* attacks successfully generated an adversarial example. The original image appears in the second row, while the top and bottom rows display color-based and diffusion-based attacks, respectively. Each caption includes the method name and the model’s predicted class.

Yuan et al., 2022)). Inspired by the ImageNet Unrestricted AEs competition (Y. Chen et al., 2021), we use images from the validation set of ImageNet-1k. However, to minimize confounding effects, we only use validation images that (i) are correctly classified with the highest confidence by the given victim model, (ii) display exactly one ImageNet object according to (Beyer, Hénaff, Kolesnikov, Zhai, & van den Oord, 2020), and (iii) do not contain any apparent modifications. Following these specific goals, we *manually* crafted a subset of relevant images for our victim model. The resulting dataset, ImageNet **SCOOTER-ResNet50-Norm** (**ImageNet S-R50-N**), contains 2966 ImageNet validation images. Appendix D provides a detailed description of the dataset creation process and an analysis of its advantages over the predominantly used dataset of the NIPS 2017 competition (Kurakin et al., 2018). With 346 complete sets of annotations, we were able to collect 17,300 ratings for ImageNet S-R50-N samples, as well as another 17,300 ratings

of adversarial images generated by six different attacks.

4.1 Experimental Setup for Color-based Attacks

The following subsections outline information about each attack’s associated experiment design. All images are generated with *untargeted* attacks, whose sole aim is to induce a misclassification – the adversary does not care which wrong label the model assigns. We ran all attacks using the parameters validated for attacking ResNet-50 on ImageNet-like data from the original papers (see Appendix C for details). We provide details about the involved participants, the compensation, and statistics regarding the time investment per person (see Tab. 6 for time commitment details). The results of these experiments will be discussed in the next section, while our supplementary material outlines additional details about the experiments (Appendix C). The top row

of Fig. 4 shows adversarial examples of all color-based attacks. In the following, we outline the experimental setup for each color-based attack.

4.1.1 Exp. 1: SemAdv – The Simple Attack

This attack is the first color-based unrestricted attack. SemAdv (Hosseini & Poovendran, 2018) tries to generate AEs by mapping images into the **HSV** color space (Smith, 1978), shifting the **Hue** and **Saturation** components while maintaining the same **Value** component.

Participants. Based on a pilot study ($n = 12$) to fix study parameters (e.g., initial sample size and estimated time commitment), we recruited 128 people via the standard Prolific sampling option. We used the preexisting Prolific filters for English fluency and colorblindness to exclude ineligible participants throughout *all three experiments*. Only 74 of the 128 invited participants completed the study without failing any checks (hence, $n = 74$). Of the 54 participant submissions we discarded as incomplete, 17 failed the colorblindness test, 16 failed the comprehension check, 5 failed at least two inattentiveness checks, 4 encountered technical issues, and 12 did not start the study (i.e., never accepted the consent form). Note that Prolific asks participants to self-report their colorblindness, which explains the non-vanishing failure rate in the colorblindness test. This explicitly shows that SCOOTER appropriately addresses self-misrepresentation (**C2**). The eligible **74** participants spent, on average, 18 minutes and 30 seconds on the entire study and 6.239 seconds per main study image.

4.1.2 Exp. 2: NCF – The Modern Attack

NCF (Yuan et al., 2022) is one of the leading color-based unrestricted attacks, performing particularly well in generating transferable AEs (i.e., images that can also fool previously unseen models). In summary, this sophisticated attack colors different segments of an image based on a realistic color distribution emanating from the ADE20k dataset (B. Zhou et al., 2017).

Participants. Based on the first experiment’s results (see Tab. 3), we collected up to 61 completed sets of annotations (this sample size

includes a buffer of $\approx 13\%$). Apart from the 61 approved submissions ($n = 61$), 6 returned their submission right away, 10 failed the colorblindness test, 14 failed the comprehension check, and 4 failed at least two attention checks. The eligible **61** participants spent, on average, 17 minutes and 56 seconds on the entire study and 6.046 seconds per main study image.

4.1.3 Exp. 3: cAdv – The Middle Ground?

Similar to NCF, cAdv (Bhattad et al., 2020) colorizes certain regions of an image based on provided image segments. However, cAdv relies on extracted coloring hints, which can then be used to maliciously recolor parts of the image using an existing colorization model.

Participants. As before, we collected 61 completed sets of annotations. Apart from the 61 approved submissions, 11 returned their submissions immediately, 19 failed the colorblindness test, 15 failed the comprehension check, and 5 failed at least two attention checks. Three participants encountered technical issues. The eligible **61** participants spent, on average, 18 minutes and 46 seconds on the entire study and 5.919 seconds per main study image.

4.1.4 Appropriate Sample Size and TOST Bounds

To estimate reliable Δ_L and Δ_U , we generated 50 million subsets of participant annotations for each attack by randomly sampling Prolific IDs. Each subset contained ratings from 50 participants for the respective experiment. The resulting simulation-wide means, $\hat{\mu}_{\text{real}}$ and $\hat{\mu}_{\text{modified}}$ (Tab. 2), in combination with the small standard deviations (see SD columns), provide multiple insights: (i) A sample size of 50 participants appears sufficient to yield robust estimates of average ratings (as illustrated by the narrow SDs); (ii) Drawing on the largest observed range of μ_{real} values, we can set practical equivalence bounds at ± 0.2 , accounting for typical fluctuations; (iii) Finally, as shown in subsequent results, the original metrics for each attack closely match these subsampled distributions, even with light variations in sample sizes and study design. This confirms that our previously empirically established study parameters are representative. All

subsequent experiments will therefore only contain annotations from 50 participants.

4.2 Experimental Setup for Diffusion-based Attacks

Based on our findings for Experiments 1-3, we also assessed three *diffusion*-based attacks as these build upon state-of-the-art image generation technologies. These attacks are DiffAttack (short: DA) (Kang et al., 2023), AdvPP (Zhang et al., 2024), and ACA (Z. Chen et al., 2023). The bottom row of Fig. 4 shows adversarial examples of all diffusion-based attacks.

Following our study design for Experiment 3 and the resulting sample size estimation, we collected 50 annotations per experiment while compensating all participants based on an average time commitment of 18 minutes and an hourly wage of £9. Because modern diffusion models can generate highly realistic images from scratch, we hypothesized that all three diffusion-based attacks would outperform their color-based counterparts. In the following, we outline the experimental setup for each diffusion-based attack.

4.2.1 Exp. 4: DA – PGD meets Diffusion

DiffAttack (DA) is a diffusion-based attack that utilizes a norm-based guiding signal stemming from the PGD attack (Madry et al., 2018) throughout intermediate diffusion steps to generate AEs. This signal is composed of norm-bounded classification loss and a supplementary deviated-reconstruction loss, ensuring that the guiding signal remains intact throughout the diffusion process.

Participants. Apart from the 50 approved submissions, 8 returned their submissions immediately, 21 failed the colorblindness test, 21 failed the comprehension check, and 4 failed at least two attention checks. Two participants encountered technical issues. The eligible 50 participants spent, on average, 19 minutes and 8 seconds on the entire study and 6.642 seconds per main study image.

4.2.2 Exp. 5: AdvPP – A Probabilistic Perspective on AEs

Zhang et al. (2024) reframe adversarial example generation as sampling from an adversarial density $p_{\text{adv}}(x) = p_{\text{vic}}(x \mid y_{\text{tar}}) p_{\text{dis}}(x \mid x_{\text{ori}})$. The victim distribution p_{vic} is an exponential of the classifier loss that drives images toward a target label, while the distance distribution p_{dis} is a data-driven generative model trained on semantics-preserving transforms or fine-tuned from a pretrained diffuser that anchors samples near the original image’s semantics.

Participants. Apart from the 50 approved submissions, 8 returned their submissions immediately, 16 failed the colorblindness test, 23 failed the comprehension check, and 5 failed at least two attention checks. Due to server issues, 14 participants experienced technical issues, and two participants prematurely quit the study. The eligible 50 participants spent, on average, 23 minutes and 36 seconds on the entire study and 8.275 seconds per main study image.

4.2.3 Exp. 6: ACA – Perturbing Latent Representations

The attack of Z. Chen et al. (2023) substantially perturbs original images to generate AEs by (i) mapping existing samples into a low-dimensional latent representation and (ii) performing adversarial perturbations on the resulting latent representation.

Participants. Apart from the 50 approved submissions, 9 returned their submissions immediately, 21 failed the colorblindness test, 28 failed the comprehension check, and 2 failed at least two attention checks. Two participants encountered technical issues. The eligible 50 participants spent, on average, 22 minutes and 50 seconds on the entire study and 8.411 seconds per main study image.

4.3 Using Vision Language Models as a Proxy for Imperceptibility

Based on our experimental design and experiences, researchers aiming to assess the imperceptibility of their attack would need to invest approximately £215 to perform a SCOOTER study (including compensation for filtered-out annotators). For this reason, we also investigated to what degree

Attack	Original Values		Sample Means		SDs ($\times 10^{-2}$)		Range of μ_{real}
	μ_{real}	$\mu_{\text{mod.}}$	$\hat{\mu}_{\text{real}}$	$\hat{\mu}_{\text{mod.}}$	$\hat{\mu}_{\text{real}}$	$\hat{\mu}_{\text{mod.}}$	
SemAdv	0.921	-1.063	0.921	-1.064	3.61	3.68	[0.748, 1.114]
cAdv	0.919	-1.674	0.919	-1.674	2.61	2.19	[0.8, 1.053]
NCF	1.029	-1.687	1.029	-1.687	2.83	2.04	[0.912, 1.174]

Table 2 Results of Subsampling Compared to the Original Values of Experiments 1-3. The table includes original and sample-wide means, as well as the standard deviation (SD) and the observed range of μ_{real} values across 50 million simulations per attack.

OpenAI’s multimodal GPT-4o model (OpenAI et al., 2024) can (i) accurately detect AEs while (ii) aligning with human annotations.

Experiment Design. Based on our participant instructions, we created a system prompt for the model to generate Likert-scale ratings for all 2,966 unaltered images, as well as the 6,924 adversarial counterparts that the six attacks successfully produced (each attack attempted to transform all 2,966 images, but many attempts failed; see Sec. 5 for details). Contrary to SCOOTER studies, the GPT-4o model evaluated each image separately and independently (i.e., the model only saw one single image per annotation request). In each request, we asked the model to only output a Likert-scale rating between -2 and +2. Due to the enforced concise output behavior, the relatively small size of images, and the text-only system prompt, our request contained, on average, 650 input tokens and exactly 3 output tokens. According to the OpenAI API pricing guidelines² (as of June 2025), assessing an image with GPT-4o would cost approximately \$0.001655. If an attack achieved a flawless success rate against the victim model – transforming every one of the 2,966 images into an adversarial example – a VLM-based evaluation would cost roughly \$4.90, compared with about £215/\$293 for a full-scale SCOOTER study. The corresponding system prompt is shown in Appendix C.6.

4.4 Objective Quality Metrics.

As discussed in our introductory sections, image generation systems, including those that create adversarial images, evaluate the quality of

their generated images using automated “objective” metrics. However, even though current systems, especially modern diffusion models, generate extremely realistic images, prior research has shown that commonly used metrics do not always align with human intuition (Stein et al., 2023). A study directly correlating these metrics with human scores from SCOOTER would clarify the existing gap and determine if insights from traditional generative-image research apply to the more challenging, security-focused domain of unrestricted adversarial examples. Therefore, we decided to leverage the existing codebase of (Stein et al., 2023) to assess the alignment of some proposed objective metrics.

Choice of Metrics and Feature Extractor. We selected a subset of metrics used in (Stein et al., 2023) based on specific criteria. First, we excluded any metrics that require an additional set of images beyond the real baseline and the generated images from the attacks (e.g., FLS). We also discarded metrics that rely on the labeling of a specific model (e.g., inception score or Vendi score). Finally, we omitted metrics that assess less relevant characteristics in the context of adversarial example generation, such as image rarity or degrees of memorization. Following the recommendation of (Stein et al., 2023), we used DINOv2 as our feature extractor instead of the commonly used Inception-V3 network.

Ranking Metrics. Many common objective quality metrics measure the difference between real and generated distributions: the closer these distributions are, the more realistic the generated images appear. Here, we will utilize the Fréchet Distance (**FD**, (Fréchet, 1957)), the kernel distance (**KD**, (Sutherland, Arbel, & Gretton, 2018)), and the proposed Sliced Wasserstein Distance (**SWD**, (Stein et al., 2023)) to quantify distribution differences based on DINOv2 (Oquab et al., 2024) features.

²<https://platform.openai.com/docs/pricing>

Sample Diversity and Fidelity. While any of the above metrics would suffice as an initial indicator of image quality, we explored additional metrics that disentangle fidelity (how realistic individual samples are) from diversity (how completely the model covers the data manifold). Following Stein et al. (2023), we again operate in the representation space of DINOv2 features to compute the four complementary PRDC metrics – Precision, Recall, Density, and Coverage:

- **Precision (Prec. \uparrow):** The fraction of generated samples that fall inside the k -nearest-neighbour hyperspheres constructed around real images. High precision means the generator stays on the manifold. Defined by (Kynkäänniemi, Karras, Laine, Lehtinen, & Aila, 2019; Sajjadi, Bachem, Lucic, Bousquet, & Gelly, 2018).
- **Recall (Rec. \uparrow):** The fraction of real images that are covered by any sphere centred on generated samples. High recall indicates the model reaches all modes of the real distribution. Defined by (Kynkäänniemi et al., 2019; Sajjadi et al., 2018).
- **Density (Den. \uparrow):** For each generated sample, we count how many real image spheres it contains and average over the set, rewarding generators that place probability mass in densely populated regions. Defined by (Naeem, Oh, Uh, Choi, & Yoo, 2020).
- **Coverage (Cov. \uparrow):** For each real image, we ask whether at least one generated sample visits its sphere; averaging these binary hits penalizes mode collapse without being sensitive to oversampling. Defined by (Naeem et al., 2020).

We adopt the original hyperparameters, $k = 5$ and sample size = 10,000, with the latter resulting in the use of all real and generated images.

Multi-Criteria Model Comparison. Inspired by (Harman, Yu, Konstantinidis, & Gonzalez, 2021), we utilize the Borda-score aggregation proposed therein to summarize attack imperceptibility across all objective metrics: for every metric, we first rank the compared attacks and translate ranks into Borda points (best = m , worst = 1, where m is the number of attacks). We then sum the Borda points across all metrics to output a single objective metric score that is scale-invariant, rewarding consistent high performance and penalizing cases where an attack excels on one metric but fails on others.

4.5 Limitations of the Study Design

Online studies generally lack control over participants' environments, which could lead to rating inconsistencies. For instance, while non-desktop participants are excluded in SCOOTER, different screen resolutions can affect human perception. Our population is also (i) younger than the OECD-wide median age of 40 (OECD, 2019) (median age: 29) and (ii) overrepresents South African citizens, with South Africa being the most common nationality across all six experiments. We highlight further demographic statistics in Appendix C.4. Additionally, a subjective interpretation of what constitutes a "modified" image can lead to variability in participant ratings despite using comprehension checks to standardize understanding. The quality of our instructions would also impact the proposed VLM-based proxy assessment, as it directly builds upon our annotation guidelines.

As we dynamically improved the study design, the comprehension check also differs between Exp. 1 and Exp. 2/3, which may introduce slight differences in initial task comprehension, potentially affecting direct comparisons between Exp. 1 and the later experiments. However, the core screening criteria and concepts remained consistent (as underscored by the consistent success rate on preliminary checks across all subsequent experiments), providing a reliable baseline for participant comprehension. Additionally, the participants in the latter two diffusion-based experiments (Exp. 5 and Exp. 6) invested, on average, more time in the annotation process compared to the other four experiments. While these outliers can be explained through the rating behavior of annotators (see Sec. 5 for details), one may still need to raise the compensation further to cover 20-22 minutes of work adequately (e.g., given our base pay of £9/hr, increase the compensation to £3.00 – £3.30).

Finally, the observed high failure rate in the two preliminary checks is surprising, especially for the colorblindness test, considering that all invited participants explicitly identified themselves as *not* colorblind. However, many participants failed to select the 'I don't see a digit' option, indicating inattentiveness rather than true colorblindness in some cases.

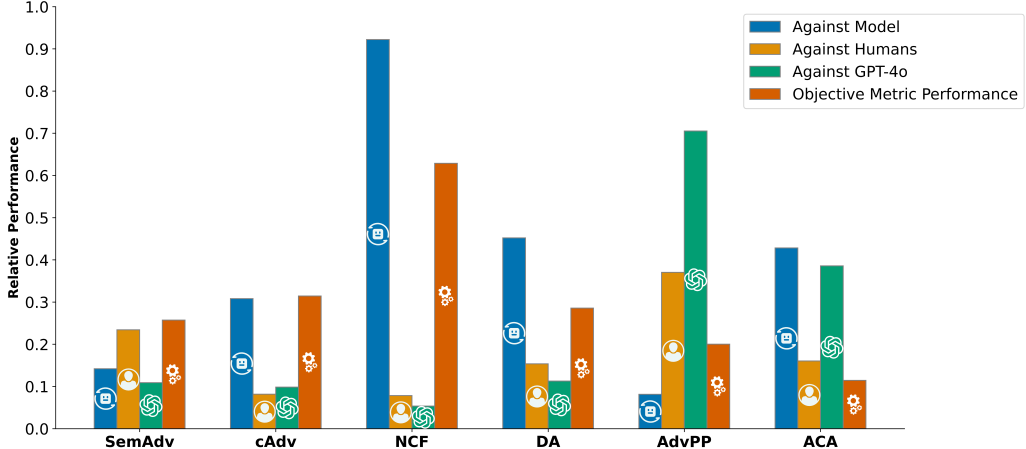


Fig. 5 Relative performance of different adversarial attack methods against our victim model (blue), human evaluators (orange), and OpenAI’s GPT-4o model (green) in terms of imperceptibility. We also visualize each attack’s cumulative performance based on the normalized Borda score of our objective metrics (dark orange). Attack success against humans is based on the μ_{modified} scores of Tab. 3, which can range from -2 (definitely modified) to $+2$ (definitely real). Here, the scores were rescaled to a $0\text{--}1$ range, where 1 indicates the highest degree of imperceptibility.

Metric	SemAdv	cAdv	NCF	DA	AdvPP	ACA
ASR \uparrow	0.142	0.3082	0.922	0.4521	0.0813	0.4282
$\mu_{\text{Modified}} \uparrow$	-1.063	-1.674	-1.687	-1.3856	-0.5188	-1.1552
μ_{Real}	0.921	0.919	1.029	1.000	0.587	0.715
Hypothesis	P-Values of Equivalence Testing via TOST ($\alpha = 0.05$)					
$\Delta < \Delta_L$	5.873e-61	1.899e-40	4.147e-44	3.039e-33	2.114e-23	1.695e-27
$\Delta > \Delta_U$	1.000	1.000	1.000	1.000	1.000	1.000

Table 3 The key metrics as described in Sec. 3.3 for the color-based and diffusion-based attacks. As described in Sec. 4, each color-based attack was tested with a significantly higher amount of samples than necessary (SemAdv: $n = 74$, cAdv: $n = 61$, NCF: $n = 61$) while the diffusion-based attacks were tested using the derived sample size of $n = 50$. The \uparrow arrow indicates that the metric should be *maximized*. The best performing attack per metric is highlighted in **bold**.

5 Results

Previous work in unrestricted attack literature has claimed that the proposed unrestricted attacks are imperceptible to the human eye. However, as summarized in Tab. 3, we have statistically significant evidence pointing to the exact opposite: Given $\alpha = 0.05$, all six tests for the null hypothesis $\Delta > \Delta_U$ failed to reach significance, indicating that real images are rated higher than the generated AEs beyond the margin of imperceptibility (± 0.2). Even the most promising attack, AdvPP, demonstrates a much wider rating gap between real and modified images. To better understand the factors driving these perceptual differences, we now turn to a series of focused analyses. Specifically, we examine: (1) whether more sophisticated attacks yield more

imperceptible adversarial examples, (2) how individual attacks compare in detail, (3) how human perception aligns with model predictions, and (4) whether objective metrics can reliably approximate human judgment.

Do Complex Attacks Outperform Simple Ones? While the more novel and complex attacks tend to outperform older, simpler ones (particularly when only comparing diffusion-based attacks), SemAdv represents an interesting exception: despite being the simplest attack, it outperforms four out of the five other attacks with an average score of -1.063 for modified images. However, taking μ_{Real} into account, one could also argue that ACA outperforms SemAdv: while SemAdv has a higher μ_{Modified} score, the lower $|\mu_{\text{Mod.}} - \mu_{\text{Real}}|$ margin of ACA indicates that the diffusion-based attack is superior to SemAdv. In

this regard, based on the results, we conclude that both attacks are comparable to one another.

Beyond SemAdv, we can deduce that cAdv modifications are *slightly* more imperceptible than NCF modifications – despite having a similar μ_{Modified} value ($| -1.674 - 0.919 | < | -1.687 - 1.029 |$). This further undermines our hypothesis. A possible explanation for this result is that NCF modifications are so apparent that participants can more easily identify when an image has **not** been altered – this would also align with the sample images presented in Fig. 4 in which the NCF sample displays prominent and unrealistic red coloring.

The Six Attacks in Detail. While we invite readers to examine our dataset for a more nuanced perspective on image quality, the samples shown in Fig. 4 highlight the core characteristics of the attacks.

For the color-space attacks, SemAdv tends to incorporate more subtle greyish coloring, while NCF and cAdv lead to more prominent modifications. NCF often applies very prominent coloring across the entire image, while cAdv mainly adds distinctive color patches to images. These characteristics are also present in the sample images of the respective paper – although less pronounced than in our dataset. Potential reasons for this discrepancy include (i) a strategic choice of sample images and (ii) the more robust adversarially trained ResNet-50 model, which may require more obstructive modifications than previously explored non-robust victim models. This would reinforce the idea that selecting a robust model yields a more demanding — and therefore more informative — imperceptibility test.

On the other end, the three diffusion-based attacks generally outperform color-based attacks (see Tab. 3). DiffAttack (DA) predominantly introduces adversarial perturbations by adjusting edges in the background of an image. While this can sometimes fool humans, it often results in either unrealistically smooth textures (as in Fig. 4) or substantial perturbations applied to written text within the image. AdvPP tends to subtly sharpen edges within images, while deforming background elements. On the other hand, AEs generated by the ACA attack represent entirely

new images that only vaguely resemble their original input image. While the attack performs relatively well against humans, it usually displays the focal object in an abstract manner (consequently, the background is substantially less detailed as seen in Fig. 4).

Beyond their relatively high modified scores, AdvPP and ACA also have an interesting impact on the perception of real images. Contrary to the other four attacks, whose μ_{real} scores hover around the +0.9 mark, AdvPP and ACA also directly *lower* the average score of our real baseline, indicating that annotators are less certain about the baseline’s image quality. This downward shift in μ_{real} not only serves as a secondary signal of higher imperceptibility (cf. our SemAdv vs. ACA comparison) but also helps explain why the last two experiments took longer: raters had to scrutinise *every* image – real as well as adversarial – more carefully before choosing a Likert score. Consequently, the average completion time increased from approximately 18–19 minutes in the first four studies to around 23 minutes for ACA and AdvPP.

Human Perception vs. Computer Vision.

Another interesting observation is the prominent performance discrepancy when attacking the victim model and human participants respectively (visualized in Fig. 5). For instance, whereas the subtle changes introduced by AdvPP rarely fool ResNet-50-AT_{norm}, NCF’s noticeable coloring completely overwhelms our robust victim model. However, this comes at the cost of imperceptibility. Our findings suggest that the attack success rate against CV models does not correlate with the imperceptibility of the modifications. Our proposed prototyping experiment via GPT-4o (see Sec. 4.3) represents an insightful middle ground: while VLM ratings do not align perfectly with the human annotations (particularly for AdvPP and ACA; see Tab. 4), they can at least serve as a rough first approximation of an attack’s imperceptibility.

While further experiments are needed, these initial findings suggest that the perception mechanisms of humans and computer vision models differ substantially (see Fig. 5), which could have profound implications for cybersecurity and computer vision, as even sophisticated multimodal

systems such as GPT-4o struggle to detect adversarial examples. We provide additional insights and statistics (including key metrics across all six sample sets) in Appendix C.

Dataset	Mean Rating	Std.	Accuracy
Real Images	1.8068	0.6329	0.9579
Color-based Attacks			
SemAdv	-0.9052	0.8952	0.8910
cAdv	-1.4087	0.9403	0.9016
NCF	-1.5020	0.6743	0.9466
Diffusion-based Attacks			
DA	-1.5095	0.9887	0.8874
AdvPP	0.4979	1.5165	0.2946
ACA	-0.6283	1.4981	0.6142

Table 4 Results of automated AE assessment via GPT-4o. Accuracy refers to the percentage of real images that received positive ratings and adversarial images that received negative ratings.

The Utility of Objective Metrics. The disparity between human perception and computer vision becomes particularly evident when comparing SCOOTER annotations with the objective metric scores presented in Tab. 5. As indicated by the overall Borda score, objective metrics rate the image quality of NCF – the least imperceptible attack – as significantly superior to that of the other attacks. The relatively low FD score of NCF is especially alarming, given that its Inception-based counterpart, FID (Heusel, Ramsauer, Unterthiner, Nessler, & Hochreiter, 2017), is commonly used as the primary metric for assessing image realism. However, NCF is not the only attack to receive an unusually high rating; the ranking of attacks is almost the direct opposite of our SCOOTER-based rankings. For instance, both NCF and cAdv are rated as the best-performing attacks, while AdvPP and ACA are positioned at the bottom of the rankings. This further reinforces the claims made by (Stein et al., 2023) and underscores the central motivation behind SCOOTER: we cannot solely depend on objective image quality metrics.

6 Conclusion

In this work, we introduced SCOOTER – a framework to assess the imperceptibility of unrestricted attacks. SCOOTER fills a long-standing methodological gap: it is the first openly available, statistically powered benchmark that links human perception to the image quality of generated adversarial examples with an empirically motivated ± 0.2 margin of imperceptibility, $> 30k$ crowd-sourced ratings, and reusable code. By replacing anecdotal “looks fine” judgments and poorly aligned objective metrics with a transparent, statistically sound human study, SCOOTER enables researchers to adequately evaluate just how imperceptible adversarial attacks are.

While previous works have claimed to produce benign-looking unrestricted adversarial examples, our benchmarking studies demonstrate the opposite: humans can easily distinguish between authentic images and those modified by unrestricted attacks. Additionally, we observe the first signs of an apparent discrepancy between human perception and the attack success rate against computer vision models (a high attack success rate does not align with high imperceptibility).

Our contributions open up an interesting avenue for future work: researchers can utilize existing SCOOTER annotations to create a more human-aligned objective metric catered explicitly to the generation of authentic adversarial examples and thus improve their imperceptibility and practicality. Although developed for unrestricted image-based attacks, researchers could also apply SCOOTER to adjacent research areas, such as image quality assessment of generative AI models. Overall, SCOOTER facilitates reproducible and statistically sound research into the imperceptibility of unrestricted attacks, setting the new standard for more human-centered adversarial attack research.

Data Availability

To facilitate research into more imperceptible, unrestricted attacks both in the short and long term, we have published all relevant, anonymized data of our SCOOTER studies. Data about the images at hand are publicly available on Zenodo under the following link: <https://doi.org/10.5281/zenodo.15771501>.

Attack	Image Quality			Sample Fidelity and Diversity				Overall Borda Score ↑
	FD ↓	KD ↓	SWD ↓	Prec. ↑	Rec. ↑	Den. ↑	Cov. ↑	
Color-based Attacks								
SemAdv	1329	0.041	0.129	0.976	0.843	1.071	0.969	16
cAdv	<u>548</u>	0.074	0.168	0.983	<u>0.913</u>	1.236	0.990	18
NCF	147	0.067	<u>0.158</u>	0.999	0.996	1.261	0.998	29
Diffusion-based Attacks								
DiffAttack	696	0.408	0.341	<u>0.997</u>	0.741	6.331	<u>0.991</u>	17
AdvPP	1865	<u>0.049</u>	<u>0.158</u>	0.958	0.813	1.394	0.983	14
ACA	793	0.235	0.261	0.986	0.671	<u>2.177</u>	0.965	11

Table 5 Full quantitative comparison of unrestricted adversarial attacks using objective metrics described in Sec. 4.4. ↑ / ↓ indicates that the metric should be maximized/minimized. The best performing attack per metric is highlighted in **bold** while the second best is underscored.

This repository includes (i) ImageNet S-R50-N and its adversarial counterparts produced by all six attacks, (ii) the human ratings per image, (iii) the ratings provided by GPT-4o, and (iv) supplementary information on how ImageNet samples were processed to create ImageNet S-R50-N.

Furthermore, our GitHub repository (see <https://github.com/DrenFazlja/SCOOTER>) includes code to process the Zenodo data. The codebase allows researchers to (i) rerun the introduced equivalence test for all six experiments, (ii) recalculate the core metrics of SCOOTER, and (iii) visualize statistics associated with the initial ImageNet S-R50-N creation process. Our codebase also enables researchers to run SCOOTER experiments using a local Flask-based web app.

Declarations

Funding. This work is supported by the Center for Digital Innovations of Lower Saxony (ZDIN) and has received funding from the Lower Saxony Ministry of Science and Culture under grant number ZN3492 (Zukunftslabor Gesellschaft & Arbeit) and through funds from the program zukunft.niedersachsen of the Volkswagen Foundation for the 'CAIMed – Lower Saxony Center for Artificial Intelligence and Causal Methods in Medicine' project (grant no. ZN4257).

Competing interests. The authors have no competing interests to declare that are relevant to the content of this article.

References

Aguinis, H., Villamor, I., Ramani, R.S.

(2021). Mturk research: Review and recommendations. *Journal of Management*, 47(4), 823-837, Retrieved from <https://doi.org/10.1177/0149206320969787>

Altman, D.G., & Bland, J.M. (1995). Statistics notes: Absence of evidence is not evidence of absence. *Bmj*, 311(7003), 485,

Bates, D., Mächler, M., Bolker, B., Walker, S. (2015). Fitting linear mixed-effects models using lme4. *Journal of Statistical Software*, 67(1), 1–48, <https://doi.org/10.18637/jss.v067.i01>

Bauer, B.W., Larsen, K.L., Caulfield, N., Elder, D., Jordan, S., Capron, D. (2020, Nov). *Review of best practice recommendations for ensuring high quality data with amazon's mechanical turk*. PsyArXiv. Retrieved from osf.io/preprints/psyarxiv/m78sf_v1

Beyer, L., Hénaff, O.J., Kolesnikov, A., Zhai, X., van den Oord, A. (2020). *Are we done with imagenet?* Retrieved from <https://arxiv.org/abs/2006.07159>

Bhattad, A., Chong, M.J., Liang, K., Li, B., Forsyth, D.A. (2020). Unrestricted adversarial examples via semantic manipulation. *International conference on learning representations*. Retrieved from https://openreview.net/forum?id=Sye_OgHFwH

Bron, A., Nicola, A.A., Blake, A., Pueyo-Bestué, A., Thomsen, A.S., Maino, A., ... Aclimandos, W. (2024). *European training requirements for the specialty of ophthalmology* (Tech. Rep.). Brussels: European Board of Ophthalmology (EBO) and Union of European Medical Specialists (UEMS) Section of Ophthalmology. Retrieved 2025-07-01, from <https://www.ebo-online.org/wp-content/uploads/FINAL-EBO-UEMS-European-Training-Requirements-for-the-Specialty-of-Ophthalmology.pdf>

Carlini, N., & Wagner, D. (2017). Towards evaluating the robustness of neural networks. *2017 ieee symposium on security and privacy (sp)* (pp. 39–57).

Chen, X., Gao, X., Zhao, J., Ye, K., Xu, C.-Z. (2023). Advdifuser: Natural adversarial example synthesis with diffusion models. *Proceedings of the ieee/cvpr international conference on computer vision* (pp. 4562–4572).

Chen, Y., Mao, X., He, Y., Xue, H., Li, C., Dong, Y., ... Yang, Z. (2021). *Unrestricted adversarial attacks on imagenet competition*. Retrieved from <https://arxiv.org/abs/2110.09903>

Chen, Z., Li, B., Wu, S., Jiang, K., Ding, S., Zhang, W. (2023). Content-based unrestricted adversarial attack. A. Oh, T. Naumann, A. Globerson, K. Saenko, M. Hardt, & S. Levine (Eds.), *Advances in neural information processing systems* (Vol. 36, pp. 51719–51733). Curran Associates, Inc. Retrieved from https://proceedings.neurips.cc/paper_files/paper/2023/file/a24cd16bc361afa78e57d31d34f3d936-Paper-Conference.pdf

Croce, F., Andriushchenko, M., Sehwag, V., Debenedetti, E., Flammarion, N., Chiang, M., ... Hein, M. (2021). Robustbench: a standardized adversarial robustness benchmark. J. Vanschoren & S. Yeung (Eds.), *Proceedings of the neural information processing systems track on datasets and benchmarks* (Vol. 1). Retrieved from https://datasets-benchmarks-proceedings.neurips.cc/paper_files/paper/2021/file/a3c65c2974270fd093ee8a9bf8ae7d0b-Paper-round2.pdf

Curran, P.G. (2016). Methods for the detection of carelessly invalid responses in survey data. *Journal of Experimental Social Psychology*, 66, 4–19.

Dai, X., Liang, K., Xiao, B. (2025). Advdif: Generating unrestricted adversarial examples using diffusion models. A. Leonardis, E. Ricci, S. Roth, O. Russakovsky, T. SatTLer, & G. Varol (Eds.), *Computer vision – eccv 2024* (pp. 93–109). Cham: Springer Nature Switzerland.

Douglas, B.D., Ewell, P.J., Brauer, M. (2023). Data quality in online human-subjects research: Comparisons between mturk, prolific, cloudresearch, qualtrics, and sona. *Plos one*, 18(3), e0279720,

Dunn, A.M., Heggestad, E.D., Shanock, L.R., Theilgard, N. (2018). Intra-individual response variability as an indicator of insufficient effort responding: Comparison to other indicators and relationships with individual differences. *Journal of Business and Psychology*, 33, 105–121,

Dziugaite, G.K., Ghahramani, Z., Roy, D.M. (2016). *A study of the effect of jpg compression on adversarial images*. Retrieved from <https://arxiv.org/abs/1608.00853>

Elsayed, G., Shankar, S., Cheung, B., Papernot, N., Kurakin, A., Goodfellow, I., Sohl-Dickstein, J. (2018). Adversarial examples that fool both computer vision and time-limited humans. S. Bengio, H. Wallach, H. Larochelle, K. Grauman, N. Cesa-Bianchi, & R. Garnett (Eds.), *Advances in neural information processing systems* (Vol. 31). Curran Associates,

Inc. Retrieved from https://proceedings.neurips.cc/paper_files/paper/2018/file/8562ae5e286544710b2e7ebe9858833b-Paper.pdf

Fazlja, D., Orlov, A., Schrader, J., Zühlke, M.-M., Rohs, M., Kudenko, D. (2024). How Real Is Real? A Human Evaluation Framework for Unrestricted Adversarial Examples. *Aaai 2024 spring symposium on user-aligned assessment of adaptive ai systems*. Retrieved from https://aair-lab.github.io/aia2024/papers/fazlja_aia24.pdf (Peer-reviewed, presented; no formal proceedings volume)

Fréchet, M. (1957). Sur la distance de deux lois de probabilité. *Annales de l'isup* (Vol. 6, pp. 183–198).

Goodfellow, I.J., Shlens, J., Szegedy, C. (2015). *Explaining and harnessing adversarial examples*. Retrieved from <https://arxiv.org/abs/1412.6572>

Göpfert, J.P., Artelt, A., Wersing, H., Hammer, B. (2020). Adversarial attacks hidden in plain sight. *Advances in intelligent data analysis xviii: 18th international symposium on intelligent data analysis, ida 2020, konstanz, germany, april 27–29, 2020, proceedings 18* (pp. 235–247).

Harman, J.L., Yu, M., Konstantinidis, E., Gonzalez, C. (2021). How to use a multicriteria comparison procedure to improve modeling competitions: A comment on erev et al.(2017). *Society for judgment and decision making; some of the ideas presented in this article were presented in an early form at the aforementioned conference*. (Vol. 128, p. 995).

He, K., Zhang, X., Ren, S., Sun, J. (2015). Deep residual learning for image recognition. *CoRR, abs/1512.03385*, , Retrieved from <http://arxiv.org/abs/1512.03385> [arXiv:1512.03385](https://arxiv.org/abs/1512.03385)

Hendrycks, D., & Dietterich, T. (2019). Benchmarking neural network robustness to common corruptions and perturbations. *International conference on learning representations*. Retrieved from <https://openreview.net/forum?id=HJz6tiCqYm>

Heusel, M., Ramsauer, H., Unterthiner, T., Nessler, B., Hochreiter, S. (2017). Gans trained by a two time-scale update rule converge to a local nash equilibrium. I. Guyon et al. (Eds.), *Advances in neural information processing systems* (Vol. 30). Curran Associates, Inc. Retrieved from https://proceedings.neurips.cc/paper_files/paper/2017/file/8a1d694707eb0fefe65871369074926d-Paper.pdf

Ho, J., Jain, A., Abbeel, P. (2020). Denoising diffusion probabilistic models. H. Larochelle, M. Ranzato, R. Hadsell, M. Balcan, & H. Lin (Eds.), *Advances in neural information processing systems* (Vol. 33, pp. 6840–6851). Curran Associates, Inc. Retrieved from https://proceedings.neurips.cc/paper_files/paper/2020/file/4c5bcfec8584af0d967f1ab10179ca4b-Paper.pdf

Hosseini, H., & Poovendran, R. (2018). Semantic adversarial examples. *Proceedings of the ieee conference on computer vision and pattern recognition workshops* (pp. 1614–1619).

Isager, P.M. (2019). *Mixed model equivalence test using R and PANGEA*. (https://pedermisager.org/blog/mixed_model_equivalence/ [Accessed: 27.01.2025])

Ishihara, S. (1917). *Tests for colour-blindness*. Tokyo, Hongo Harukichō: Handaya.

Jackson, D. (1976). The appraisal of personal reliability. *meetings of the society of multivariate experimental psychology, university park, pa*.

Johnson, J.A. (2005). Ascertaining the validity of individual protocols from web-based personality inventories. *Journal of research in personality*, 39(1), 103–129,

Joshi, A., Mukherjee, A., Sarkar, S., Hegde, C. (2019). Semantic adversarial attacks: Parametric transformations that fool deep classifiers. *Proceedings of the ieee/cvf international conference on computer vision* (pp. 4773–4783).

Judd, C.M., Westfall, J., Kenny, D.A. (2012). Treating stimuli as a random factor in social psychology: A new and comprehensive solution to a pervasive but largely ignored problem. *Journal of Personality and Social Psychology*, 103(1), 54–69, Retrieved from <https://doi.org/10.1037/a0028347>

Kang, M., Song, D., Li, B. (2023). DiffAttack: Evasion Attacks Against Diffusion-Based Adversarial Purification. A. Oh, T. Naumann, A. Globerson, K. Saenko, M. Hardt, & S. Levine (Eds.), *Advances in Neural Information Processing Systems* (Vol. 36, pp. 73919–73942). Curran Associates, Inc. Retrieved from https://proceedings.neurips.cc/paper_files/paper/2023/file/ea0b28cbbd0cbc45ec4ac38e92da9cb2-Paper-Conference.pdf

Kurakin, A., Goodfellow, I., Bengio, S., Dong, Y., Liao, F., Liang, M., ... others (2018). Adversarial attacks and defences competition. *The nips'17 competition: Building intelligent systems* (pp. 195–231).

Kynkäänniemi, T., Karras, T., Laine, S., Lehtinen, J., Aila, T. (2019). Improved precision and recall metric for assessing generative models. H. Wallach, H. Larochelle, A. Beygelzimer, F. d'Alché-Buc, E. Fox, & R. Garnett (Eds.), *Advances in neural information processing systems* (Vol. 32). Curran Associates, Inc. Retrieved from https://proceedings.neurips.cc/paper_files/paper/2019/file/0234c510bc6d908b28c70ff313743079-Paper.pdf

Laidlaw, C., Singla, S., Feizi, S. (2021). Perceptual adversarial robustness: Defense against unseen threat models. *International conference on learning representations*. Retrieved from <https://openreview.net/forum?id=dFwBosAcJkN>

Lakens, D. (2022). *Improving your statistical inferences*. Retrieved from https://lakens.github.io/statistical_inferences/ (Retrieved 2022)

Li, L., Xie, T., Li, B. (2023). SoK: Certified Robustness for Deep Neural Networks. *2023 ieee symposium on security and privacy (sp)* (p. 1289-1310).

Likert, R. (1932). A technique for the measurement of attitudes. *Archives of Psychology*, 22(140), 1–55,

Linhardt, L., Morik, M., Bender, S., Borras, N.E. (2024). An analysis of human alignment of latent diffusion models. *Iclr 2024 workshop on representational alignment*. Retrieved from <https://openreview.net/forum?id=PFnoxcKh33>

Liu, F., Zhang, C., Zhang, H. (2023). Towards transferable unrestricted adversarial examples with minimum changes. *2023 ieee conference on secure and trustworthy machine learning (satml)* (pp. 327–338).

Lyakhov, D. (2020). *Ishihara blind test cards*. <https://www.kaggle.com/datasets/dupeljan/ishihara-blind-test-cards>. ([Dataset], Kaggle username: dupeljan)

Madry, A., Makelov, A., Schmidt, L., Tsipras, D., Vladu, A. (2018). Towards deep learning models resistant to adversarial attacks. *International conference on learning representations*. Retrieved from <https://openreview.net/forum?id=rJzIBfZAb>

Mahalanobis, P.C. (2018). On the generalized distance in statistics. *Sankhyā: The Indian Journal of Statistics, Series A* (2008-), 80, S1–S7,

Modas, A., Moosavi-Dezfooli, S.-M., Frossard, P. (2019). Sparsefool: a few pixels make a big difference. *Proceedings of the ieee/cvpr conference on computer vision and pattern recognition* (pp. 9087–9096).

Na, D., Ji, S., Kim, J. (2022). Unrestricted black-box adversarial attack using gan with limited queries. *European conference on computer vision* (pp. 467–482).

Naeem, M.F., Oh, S.J., Uh, Y., Choi, Y., Yoo, J. (2020). Reliable fidelity and diversity metrics for generative models. *International conference on machine learning* (pp. 7176–7185).

OECD (2019). *Working better with age*. Paris: OECD Publishing.

OpenAI, Achiam, J., Adler, S., Agarwal, S., Ahmad, L., Akkaya, I., ... Zoph, B. (2024). *Gpt-4 technical report*. Retrieved from <https://arxiv.org/abs/2303.08774>

Oquab, M., Darcet, T., Moutakanni, T., Vo, H., Szafraniec, M., Khalidov, V., ... Bojanowski, P. (2024). *Dinov2: Learning robust visual features without supervision*. Retrieved from <https://arxiv.org/abs/2304.07193>

Otani, M., Togashi, R., Sawai, Y., Ishigami, R., Nakashima, Y., Rahtu, E., ... Satoh, S. (2023). Toward verifiable and reproducible human evaluation for text-to-image generation. *Proceedings of the ieee/cvpr conference on computer vision and pattern recognition* (pp. 14277–14286).

Prolific (2025). *Prolific*. <https://www.prolific.com/>. ([Accessed 3-7-2025])

Qiu, H., Xiao, C., Yang, L., Yan, X., Lee, H., Li, B. (2020). Semanticadv: Generating adversarial examples via attribute-conditioned image editing. *Computer vision–eccv 2020: 16th european conference, glasgow, uk, august 23–28, 2020, proceedings, part xiv 16* (pp. 19–37).

Recht, B., Roelofs, R., Schmidt, L., Shankar, V. (2019). Do imagenet classifiers generalize to imagenet? *International conference on machine learning* (pp. 5389–5400).

Russakovsky, O., Deng, J., Su, H., Krause, J., Satheesh, S., Ma, S., ... Fei-Fei, L. (2015). ImageNet Large Scale Visual Recognition Challenge. *International Journal of Computer Vision (IJCV)*, 115(3), 211–252, <https://doi.org/10.1007/s11263-015-0816-y>

Sajjadi, M.S.M., Bachem, O., Lucic, M., Bousquet, O., Gelly, S. (2018). Assessing generative models via precision and recall. S. Bengio, H. Wallach, H. Larochelle, K. Grauman, N. Cesa-Bianchi, & R. Garnett (Eds.), *Advances in neural information processing systems* (Vol. 31). Curran Associates, Inc. Retrieved from https://proceedings.neurips.cc/paper_files/paper/2018/file/f7696a9b362ac5a51c3dc8f098b73923-Paper.pdf

Salman, H., Ilyas, A., Engstrom, L., Kapoor, A., Madry, A. (2020). Do Adversarially Robust ImageNet Models Transfer Better? H. Larochelle, M. Ranzato, R. Hadsell, M.F. Balcan, & H. Lin (Eds.), *Advances in Neural Information Processing Systems* (Vol. 33, pp. 3533–3545). Curran Associates, Inc. Retrieved from https://proceedings.neurips.cc/paper_files/paper/2020/file/24357dd085d2c4b1a88a7e0692e60294-Paper.pdf

Schuirmann, D.J. (1987). A comparison of the two one-sided tests procedure and the power approach for assessing the equivalence of average bioavailability. *Journal of pharmacokinetics and biopharmaceutics*, 15, 657–680,

Shamsabadi, A.S., Oh, C., Cavallaro, A. (2020). Edgefool: an adversarial image enhancement filter. *Icassp 2020-2020 ieee international conference on acoustics, speech and signal processing* (pp. 5389–5400).

processing (icassp) (pp. 1898–1902).

Shamsabadi, A.S., Sanchez-Matilla, R., Cavallaro, A. (2020). Colorfool: Semantic adversarial colorization. *Proceedings of the icee/cvpr conference on computer vision and pattern recognition* (pp. 1151–1160).

Sharif, M., Bhagavatula, S., Bauer, L., Reiter, M.K. (2019). A general framework for adversarial examples with objectives. *ACM Transactions on Privacy and Security (TOPS)*, 22(3), 1–30,

Sielmann, K., & Stelldinger, P. (2023). Adversarial perturbations straight on jpeg coefficients. *Dagm german conference on pattern recognition* (pp. 558–573).

Smith, A.R. (1978). Color gamut transform pairs. *ACM Siggraph Computer Graphics*, 12(3), 12–19,

Sohl-Dickstein, J., Weiss, E., Maheswaranathan, N., Ganguli, S. (2015). Deep unsupervised learning using nonequilibrium thermodynamics. *International conference on machine learning* (pp. 2256–2265).

Song, Y., Shu, R., Kushman, N., Ermon, S. (2018). Constructing Unrestricted Adversarial Examples with Generative Models. S. Bengio, H. Wallach, H. Larochelle, K. Grauman, N. Cesa-Bianchi, & R. Garnett (Eds.), *Advances in Neural Information Processing Systems* (Vol. 31). Curran Associates, Inc. Retrieved from https://proceedings.neurips.cc/paper_files/paper/2018/file/8cea559c47e4fbdb73b23e0223d04e79-Paper.pdf

Stein, G., Cresswell, J., Hosseinzadeh, R., Sui, Y., Ross, B., Villegas, V., ... Loaiza-Ganem, G. (2023). Exposing flaws of generative model evaluation metrics and their unfair treatment of diffusion models. A. Oh, T. Naumann, A. Globerson, K. Saenko, M. Hardt, & S. Levine (Eds.), *Advances in Neural Information Processing Systems* (Vol. 36, pp. 3732–3784). Curran Associates, Inc. Retrieved from https://proceedings.neurips.cc/paper_files/paper/2023/file/0bc795afae289ed465a65a3b4b1f4eb7-Paper-Conference.pdf

Sutherland, J., Arbel, M., Gretton, A. (2018). Demystifying mmd gans. *international conference for learning representations* (Vol. 6).

Szegedy, C., Zaremba, W., Sutskever, I., Bruna, J., Erhan, D., Goodfellow, I., Fergus, R. (2014). *Intriguing properties of neural networks*. Retrieved from <https://arxiv.org/abs/1312.6199>

Tsipras, D., Santurkar, S., Engstrom, L., Ilyas, A., Madry, A. (2020). From imagenet to image classification: Contextualizing progress on benchmarks. *International conference on machine learning* (pp. 9625–9635).

Ward, M., & Meade, A.W. (2023). Dealing with careless responding in survey data: Prevention, identification, and recommended best practices [Journal Article]. *Annual Review of Psychology*, 74(Volume 74, 2023), 577–596, Retrieved from <https://www.annualreviews.org/content/journals/10.1146/annurev-psych-040422-045007>

Wong, E., Schmidt, F.R., Kolter, J.Z. (2019). Wasserstein adversarial examples via projected sinkhorn iterations. K. Chaudhuri & R. Salakhutdinov (Eds.), *Proceedings of the 36th international conference on machine learning, ICML 2019, 9-15 june 2019, long beach, california, USA* (Vol. 97, pp. 6808–6817). PMLR. Retrieved from <http://proceedings.mlr.press/v97/wong19a.html>

Xiang, T., Liu, H., Guo, S., Gan, Y., Liao, X. (2022, nov). Egm: An efficient generative model for unrestricted adversarial examples. *ACM Trans. Sen. Netw.*, 18(4), , <https://doi.org/10.1145/3511893> Retrieved from <https://doi.org/10.1145/3511893>

Xu, W., Evans, D., Qi, Y. (2018). Feature squeezing: Detecting adversarial examples in deep

neural networks. *Network and Distributed Systems Security Symposium (NDSS)*, ,

Xue, H., Araujo, A., Hu, B., Chen, Y. (2023). Diffusion-Based Adversarial Sample Generation for Improved Stealthiness and Controllability. A. Oh, T. Naumann, A. Globerson, K. Saenko, M. Hardt, & S. Levine (Eds.), *Advances in Neural Information Processing Systems* (Vol. 36, pp. 2894–2921). Curran Associates, Inc. Retrieved from https://proceedings.neurips.cc/paper_files/paper/2023/file/088463cd3126aef2002ffc69da42ec59-Paper-Conference.pdf

Yang, L., Song, Q., Wu, Y. (2021). Attacks on state-of-the-art face recognition using attentional adversarial attack generative network. *Multimedia tools and applications*, 80, 855–875,

Yuan, S., Zhang, Q., Gao, L., Cheng, Y., Song, J. (2022). Natural Color Fool: Towards Boosting Black-box Unrestricted Attacks. S. Koyejo, S. Mohamed, A. Agarwal, D. Belgrave, K. Cho, & A. Oh (Eds.), *Advances in Neural Information Processing Systems* (Vol. 35, pp. 7546–7560). Curran Associates, Inc. Retrieved from https://proceedings.neurips.cc/paper_files/paper/2022/file/31d0d59fe946684bb228e9c8e887e176-Paper-Conference.pdf

Zhang, A., Zhang, M., Wischik, D. (2024). Constructing Semantics-Aware Adversarial Examples with a Probabilistic Perspective. A. Globerson et al. (Eds.), *Advances in Neural Information Processing Systems* (Vol. 37, pp. 136259–136285). Curran Associates, Inc. Retrieved from https://proceedings.neurips.cc/paper_files/paper/2024/file/f620c653a8f196076f9a2fbc3c9d7efb-Paper-Conference.pdf

Zhao, Z., Liu, Z., Larson, M. (2020). Towards large yet imperceptible adversarial image perturbations with perceptual color distance. *Proceedings of the ieee/cuf conference on computer vision and pattern recognition* (pp. 1039–1048).

Zhou, B., Zhao, H., Puig, X., Fidler, S., Barriuso, A., Torralba, A. (2017). Scene parsing through ade20k dataset. *Proceedings of the ieee conference on computer vision and pattern recognition* (pp. 633–641).

Zhou, S., Gordon, M., Krishna, R., Narcomey, A., Fei-Fei, L.F., Bernstein, M. (2019). HYPE: A Benchmark for Human eYe Perceptual Evaluation of Generative Models. H. Wallach, H. Larochelle, A. Beygelzimer, F.d. Alché-Buc, E. Fox, & R. Garnett (Eds.), *Advances in Neural Information Processing Systems* (Vol. 32). Curran Associates, Inc. Retrieved from https://proceedings.neurips.cc/paper_files/paper/2019/file/65699726a3c601b9f31bf04019c8593c-Paper.pdf

Zygomatic (2025). *Photofilters*. <https://www.photofilters.com/>. ([Accessed 6-7-2025])

A Communication Sample Texts

We provide text templates that researchers should repurpose for their experiments to streamline and standardize communication with participants and researchers. The following templates follow best practices and are often based on existing literature.

A.1 Communication with Participants

This section covers every form of communication with participants, from the initial posting of the user study to instructions within the SCOOTER annotation pipeline. However, this section will only highlight the provided text — not any example images or UI components. The UI components and example images used within the templates below are part of the codebase.

A.1.1 Online Listing of Study

This subsection briefly outlines the core parameters of our Prolific task listing. Information includes the external study name, description, device requirements, and chosen study labels.

Study Name: How good are you at detecting modified images?

Device Requirements: Desktop

Study Labels: Annotation, Content Warning – *Exposure to explicit or disturbing content*

Study Description: This study aims to learn how humans judge the realism of images modified by AI (Artificial Intelligence) systems. Your task is to assess different images based on their realism (i.e., is the given image real or modified?). Please assume that every real image represents an unmodified photograph of a real-world object. With your input, you will contribute to the reliability and safety of future image-processing AI systems.

Important: We require all participants to have no form of color blindness and to be fluent in English! Please turn up the brightness of your screen to 100% and deactivate screen filters (e.g., blue light filter). We also recommend removing eyewear with colored lenses. Additionally, this is a desktop-only study.

Payment: You will receive your reward within 24-48 hours.

Optional Disclaimer:

Work in Progress: We continue to work on and improve the study platform, so you may encounter some technical issues. Please reach out to us with any comments and feedback!

A.1.2 Consent Form

Disclaimer: The following template directly builds upon Appendix G of ([Aguinis et al., 2021](#)).

This study's purpose is to learn how humans judge the realism of images modified by AI (Artificial Intelligence) systems. Your task is to assess different images based on their realism (i.e., is the given image real or modified?). Please assume that every real image represents an unmodified photograph of a real-world object. With your input you will contribute to the reliability and safety of future image-processing AI systems. To participate, you must be **at least 18 years of age**. Your participation should take about **18 minutes** and you must complete it in one sitting. You must complete this task on a **laptop or desktop computer**. Although it may not directly benefit you, this study may benefit society by improving our knowledge on the shortcomings of AI systems for images. There are no risks for participating in this study beyond those associated with normal computer use. If you complete the study, you will receive **compensation** to compensate you for your participation. You will be paid via **crowdsourcing service's** payment system. Please note that this study contains several checks to make

sure that participants are finishing the tasks honestly and completely. In accordance with the policies set by **crowdsourcing service**, we may reject your work if you do not complete the task correctly or if you do not follow the relevant instructions. Please understand that your participation is voluntary, and you have the right to withdraw your consent or discontinue participation at any time without penalty. To stop, click on the “Return Task” button, or close your browser window. Your responses will be confidential and can be identified only by your **crowdsourcing service** ID number, which will be kept confidential and will not appear in any reports or publications of this study. All your responses will only be analyzed and reported at a group level. You may print this form for your records. If you have questions about this research study or your participation, please contact **Name, Institute** by email at **e-mail-address**. Thank you very much for your participation.

By clicking the “I consent” button below, you indicate that you are 18 years of age or older, that you have read and understood the description of the study, and that you agree to participate. You also agree to our Privacy Policy and our Cookie Policy.

Warning: This is the only time we will provide you the print option on this website. Please contact **e-mail-address** if you would like to receive the consent form at a later point.

A.1.3 Colorblindness Test Description

Before we start the study, please complete a quick (approx. 30 seconds) test to check your ability to see different colors. To ensure accuracy, turn up your screen brightness to 100% and deactivate any screen filters (e.g., blue light filter). We also recommend removing eyewear with colored lenses. You will be shown images of different digits and asked to select the correct one. **If you cannot see a digit, be sure to select the "I don't see a digit" option.**

Warning: Failing this test will result in you not being able to continue the study and you will only be compensated for **30 seconds of work**.

A.1.4 Comprehension Check Description

Read the following explanations carefully.

Task: Rate images based on how modified they appear. Real/Unmodified images are photographs captured using cameras or other imaging devices, showing scenes or objects as they naturally exist. Modified images have been edited in any form, such as using Instagram/Snapchat filters, (partially) recoloring pictures, or adding/removing objects in a photo.

Two example images: An unmodified image and the same image modified via a social media filter.

Images with **defective (“dead”)** pixels or other pixel changes should be rated as “modified.”

Two example images: An unmodified image and the same image modified with strong noise.

Images with consistent but **unusual or unnatural coloring** should also be rated as “modified,” such as greyscaled images.

Two example images: An unmodified image and the same image but greyscaled

Images with **non-color related modifications** like unusually sharp edges and lines should be rated as “modified.”

Two example images: An unmodified image and the same image but with sharper edges

Rule of thumb #1: If an image looks like it's straight out of a camera without filters, it's likely unmodified.

Some edited images may have minimal and subtle signs of modifications, like inconsistent coloring or unusual lines.

Two example images: An unmodified image and the same image but with subtle changes.

Rule of thumb #2: Some modifications are obvious, while others are hard to notice.

Image Quality: The images you'll assess were made in the early 2000s, so the quality might be lower than you're used to. Also, some images were taken indoors without natural light, affecting their quality. For example, the image below is real, but due to artificial lighting, **describe unusual features**, e.g., **yellowish coloring stemming from unnatural light sources**.

Single example image in line with above description.

Rule of thumb #3: Some real images may not be as clear as you're used to. Real indoor images may have unnatural colors due to artificial lighting.

On the next page, you'll get some examples to test your understanding of the task.

Important: After the comprehension check, you'll only be shown one image. You must decide whether it's real or modified.

Next page.

We will now test whether you understood the instructions from the previous page. Of course, you can go back to the previous page to re-read the instructions by clicking the "Go Back to Instructions" button on the left hand side of your screen. For this purpose, we will show you six image pairs. For each pair, you will have to decide which of the two is a modified image. Each pair consists of one real image and one modified image. For each of the six pairs below, please select the image you believe to be **modified**. Please do this for each pair. You will be able to change your answers until you press the "Submit" button. Once you have submitted your answer, you will not be able to change it.

Warning: Failing to correctly classify **at least 5 out of the 6 pairs** will disqualify you from participating in the main study (though, we will compensate you for **6 minutes of work**). Please take your time and make sure you understand the instructions.

Beginning of the comprehension check.

A.1.5 Main Study Description

You are about to start the main study, which will take approximately **11 $\frac{1}{2}$ minutes**. You will be asked to rate the degree of image modification for **106 images**. Ensure you have a stable internet connection. If disconnected, you can restart the study via the **crowdsourcing service** URL and continue from where you left off after giving your consent again. Unlike the previous test, you will now rate each image on a 5-point scale from "Definitely Modified" to "Definitely Real." The images will appear in random order. Correctly rating more images will improve your position on our leaderboard, which you can join after the test. A rating is "correct" if it falls in the correct half of the scale (e.g., if the image is modified, you should rate it as "Definitely/Probably **Modified**"; if not modified, rate it as "Definitely/Probably **Real**"). The scale is shown below.

Screenshot of the annotation user interface.

Warning: This study includes attention checks! Failing more than one will result in a significantly lower payout.

If unsure, you can select "Unsure" to skip to the next image or use the green arrow buttons to navigate between images. At the top of the screen, you can see which images have been rated and how many are left. Blue dots indicate rated images, while grey dots show images left to rate. You can jump to an image by clicking on the respective dot. See the example below.

Screenshot of the completion bar interface.

A.2 Results Communication

A.2.1 Sample Text

We used the SCOOTER framework to assess the attack's imperceptibility and demonstrate the image quality of AEs produced by our attack. Following the guidelines and recommendations of \citet, we gathered 50 complete annotations for our attack. We filtered out m additional participants due to failing (i) the colorblindness test (x/m), (ii) the comprehension check (y/m), or (iii) due to triggering inattentiveness flags of SCOOTER (z/m). Tables XX and YY summarize our experiment's key SCOOTER metrics and time statistics. In line with existing guidelines, participants were paid **total amount per person** for 18 minutes of work (**rate-per-hour**) for successfully completing the study. We compensated filtered-out participants based on their invested time and the recommendations of \citet. As suggested by \citet, we perform an equivalence test using the two-one-sided tests (TOST) procedure \cite{tost} with the recommended practical equivalence bounds of ± 0.2 .

A.2.2 Additional Information to Report

In addition to the metrics outlined in the sample text, researchers should report their participants' core demographic data. While it is challenging to incorporate all demographic statistics into the main part of a manuscript, researchers should at least outline some demographic information, like age and sex/gender, and add the remaining statistics as supplementary material. We also highly recommend that researchers outline the limitations of their study (especially regarding potential demographic biases), as it is the absolute standard in study-based research. For instance, even with SCOOTER being constantly optimized, some general downsides of online studies (e.g., lacking control of the participant's environment) will remain.

B Adjustable SCOOTER Parameters

Many study design parameters, such as the number of main study images or the inattentiveness thresholds, are fixed parameters of SCOOTER. However, two suggested parameter instantiations, the number of Ishihara-like images and the total compensation, can be adjusted if needed.

For instance, we chose the number of Ishihara-like images simply due to the design of the corresponding Kaggle dataset (Lyakhov, 2020): the images are associated with one of four colorization types (as visualized in Fig. 6). As such, we decided to check each colorization type once and add an "empty image" (i.e., an image without a digit), leading to a total of five test images per person. The empty image colorization type is chosen randomly.

Researchers should constantly adjust participants' compensation based on financial developments (most notably inflation) and up-to-date guidelines of crowdsourcing services and the research community. As of November 2024, Prolific highly recommends that researchers compensate participants for an average of £9 per hour. Based on an average completion time of 18 minutes and completion times per study phase, successful participants would receive £2.70. We paid inattentive participants as follows: Participants who failed the colorblindness test received £0.10 (30 seconds of work), those who failed the comprehension

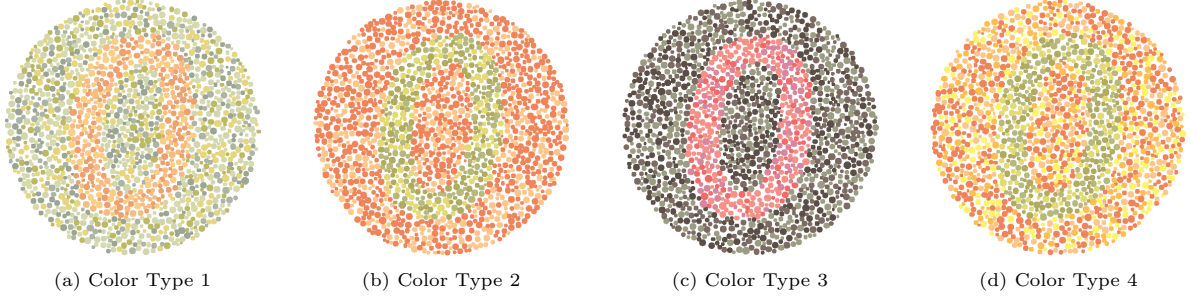


Fig. 6 All four colorization types for a single digit-font pair (digit = zero, font = Asap Medium Italic) of (Lyakhov, 2020).

check received £0.90 (6 minutes of work), and inattentive workers of the main study received £1.73 (11.5 minutes of work).

C Experiment Details

C.1 Attack Parameters.

SemanticAdv. The only parameter of the attack is the number of trials N . Based on the findings of (Hosseini & Poovendran, 2018), we also generated AEs by setting $N = 1000$.

cAdv. Bhattad et al. (2020) outline multiple parameters impacting the attack success rate and image quality of cAdv images. Based on their comments (and the default parameters of their open-source code), we used the best-performing combination of parameters (we refer the reader to the original paper for details about the parameters): Number of clusters for K-Means based segmentation: 8, Number of segments the adversary modifies: 4, Number of input hints forwarded to the colorization network: 50, Learning rate of Adam Optimizer: 10^{-4} .

NCF. In line with the original paper’s implementation details (Yuan et al., 2022), we used the following setup (we refer the reader to the original paper for details about the parameters): segmentation model: Swin-T, color distribution library size $M = 150$, the number of random searches $\eta = 50$, the iteration of neighborhood search $N = 15$, the maximum perturbation of transfer matrix $\epsilon = 0.2$, the step size $\alpha = 0.013$, the momentum $u = 0.6$, and the reset number $K = 10$.

DiffAttack (DA). All AEs generated via SCOOTER build upon the standard implementation of DA, i.e., we did not employ any further optimization using the supplementary pseudo mask. This enables us to make fair comparisons with the other standardized attack implementations. We performed the attack with the default parameters for the total DDIM sampling steps (20), the starting step of the attack (15), the number of iterations to optimize the AE (30), the resized resolution (224×224), the guidance scale of the diffusion model (2.5), the attack loss weight factor (10), the cross attention loss weight factor (10,000) and the self attention loss weight factor (100).

AdvPP. We used both the provided fine-tuning and adversarial density sampling scripts with their default parameters. Specifically, we generate each 256×256 -pixel adversarial image using a class-conditional diffusion model that follows the full 1,000-step noise schedule, but resamples only every fourth step (250 evaluations), starting at step 150 to skip the noisiest phases. The U-Net backbone utilizes 256 base channels, 64-channel multi-head attention at 32, 16, and 8-pixel resolutions, two residual blocks per scale, scale-shift normalization, and residual up-down links. Training proceeds with a learning rate of 1×10^{-6} , a batch size of 1, and checkpoints are saved every 300 steps. The model learns its own σ schedule. At inference, we draw a single sample per run, guided by a class label and a classifier scale

of 5.0. Computations are performed in full precision (FP32) under a linear noise schedule.

ACA. For the ACA attack, we keep the exact default settings provided by the authors' public code. Each image is perturbed for 10 optimisation steps in the Stable-Diffusion latent space, using an L2 loss with step size $\alpha = 0.04$, mean-squared-error weight $\beta = 0.1$, momentum $\mu = 1$, and an overall latent-space budget of $\varepsilon = 0.1$. Sampling follows the paper's 50-step DDIM schedule (β starting at 0.00085 and ending at 0.012, with a scaled-linear progression), using a classifier-free guidance scale of 7.5.

C.2 Time Statistics per Experiment

Table 6 contains all vital statistics about the time commitment per participant. While we included this information primarily for transparency, Tab. 6 offers the following valuable supplementary insights:

1. The time metrics justify our compensation guidelines, demonstrating that payment based on 18 minutes of work is reasonable and fair.
2. The consistency of time metrics across experiments validates our study design – minor adjustments made throughout the first three experiments do not significantly impact the invested time of a participant.

C.2.1 Time Statistics for Preliminary Checks.

SemAdv. The median colorblindness test time of participants who completed the check successfully ($n = 90$) is 21s and 594ms and the median comprehension check time of participants who reached the main study ($n = 74$) is 03:58 minutes.

NCF. The median colorblindness test time of participants who completed the check successfully ($n = 75$) is 20s and 398ms and the median comprehension check time of participants who reached the main study ($n = 61$) is 04:20 minutes.

cAdv. The median colorblindness test time of participants who completed the check successfully ($n = 76$) is 19s and 942ms and the median comprehension check time of participants who reached the main study ($n = 61$) is 03:07 minutes.

DiffAttack (DA). The median colorblindness test time of participants who completed the check successfully ($n = 71$) is 22s and 590ms and the median comprehension check time of participants who reached the main study ($n = 50$) is 03:38 minutes.

AdvPP. The median colorblindness test time of participants who completed the check successfully ($n = 73$) is 22 and 320ms and the median comprehension check time of participants who reached the main study ($n = 50$) is 04:17 minutes.

ACA. The median colorblindness test time of participants who completed the check successfully ($n = 78$) is 24 and 824ms and the median comprehension check time of participants who reached the main study ($n = 50$) is 04:01 minutes.

C.3 Changes made throughout Experiments

As mentioned in Sec. 4.1, we iteratively incorporated feedback to make minor study design changes throughout our series of color-space experiments. Such changes include (i) adjustments made to the compensation, (ii) user interface changes, and (iii) changes to the comprehension check.

Compensation Adjustments. Before Experiment 1, we assumed that participants would, on average, need around 15 minutes to complete the study. Hence, we compensated participants who completed

Measure	SemAdv	cAdv	NCF	DA	AdvPP	ACA
Sample Size	74	61	61	50	50	50
(i) Total Time Needed (in minutes)						
Average	18:30	17:56	18:46	19:08	23:36	22:50
Standard Dev.	7:39	8:35	7:36	7:08	11:35	9:18
Median	16:46	16:03	18:29	17:19	21:33	20:54
Minimum	7:56	7:44	05:29	8:09	5:54	7:22
Maximum	40:47	44:16	41:53	35:35	52:21	48:07
(ii) Time per Main Study Image (in seconds)						
Average	6.239	6.046	5.919	6.642	8.275	8.411
Standard Dev.	2.481	2.857	2.649	2.742	4.081	3.928
Median	5.545	5.192	5.657	6.092	7.374	7.521
Minimum	2.778	2.297	1.989	2.625	2.732	2.588
Maximum	12.784	13.580	14.268	15.126	20.297	21.052

Table 6 An overview of observed time commitments across all experiments of Sec. 4. The overview includes statistics about (i) the study completion time and (ii) the annotation time per main study image.

the study with £2.25 (£9/hr). Participants who failed the colorblindness check received £0.15 (1 minute of work), those who failed the comprehension check received £0.75 (5 minutes of work), and inattentive participants of the main study received £1.50 (10 minutes of work). For Experiment 2, we paid for an average completion time of 17 minutes (£2.55). Participants who failed the colorblindness check received £0.10 (Prolific minimum, 30 seconds of work), those who failed the comprehension check received £0.82 (5.5 minutes of work), and inattentive participants of the main study received £1.65 (11 minutes of work). Finally, Experiment 3 followed our current recommendation of compensating for 18 minutes of work (£2.70). Participants who failed the colorblindness check received £0.10 (Prolific minimum, 30 seconds of work), those who failed the comprehension check received £0.90 (6 minutes of work), and inattentive participants of the main study received £1.73 (11.5 minutes of work). We paid participants with technical issues throughout all six experiments based on their invested time.

Minor Improvements of the User Interface. Many participants of our first experiment failed the colorblindness check because they never chose the "I don't see a digit" option. As such, we slightly adjusted the related instructions to emphasize the existence of said option. We also added new examples to the comprehension check explanation while shortening the related descriptions. Finally, prior to starting Experiment 2, we also slightly increased the size of the Likert scale radio buttons. Based on feedback from Experiment 2 participants, we then increased the width of the comprehension check image pair preview so that the images appear larger (a zoom-in button per image was also always available).

Changes made to the Comprehension Check. Owing to the high drop-out rate at Experiment 1's comprehension check, we removed instances of modified and real images that were too difficult. Concretely, we removed all real images that were misclassified at least thrice and all modified images that were misclassified at least twice. As such, the six comprehension check pairs of Experiments 2 and 3 were sampled from 23 real images and 86 modified images. Despite these adjustments, the core screening criteria and concepts remained consistent across all experiments. Additionally, the consistent success rate observed across Experiments 2 and 3 indicates that participant comprehension was reliably maintained. Therefore, we believe the impact on the final results to be insignificant.

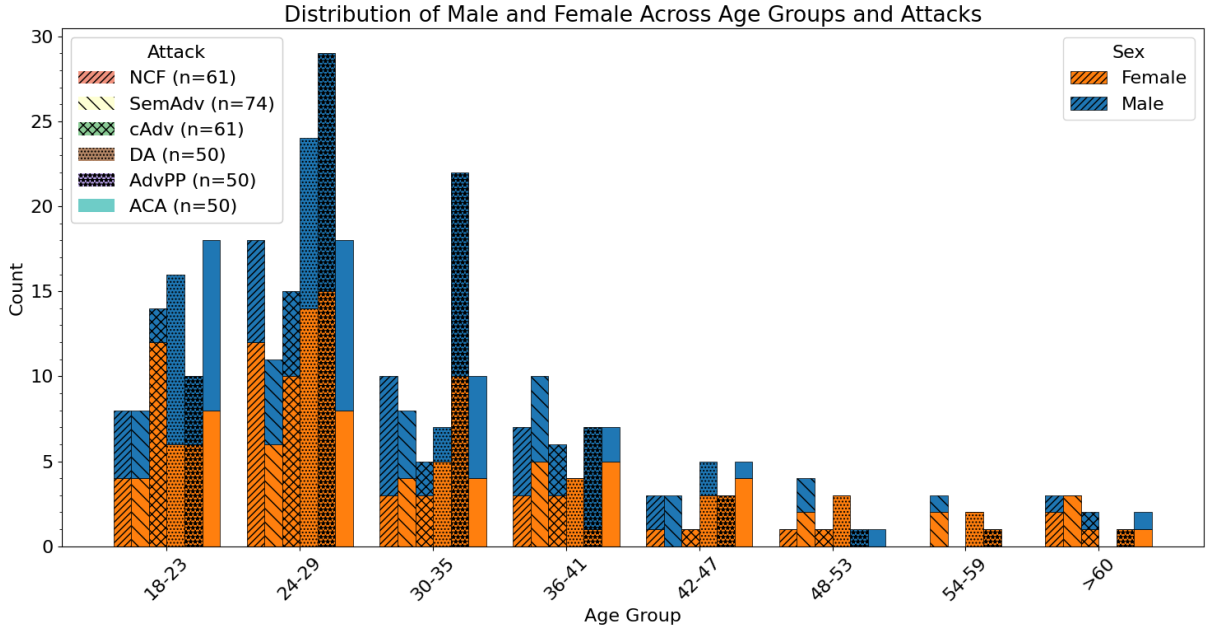


Fig. 7 Visual Comparison between Sex and Age Groups across all six Attacks. The hatch patterns on the bars indicate the assessed attack, while the height of the bars visualizes the number of male (blue) and female (orange) participants of the respective age groups.

C.4 Demographic Statistics

Prolific allows researchers to export core demographic information about their participants. As of June 2025, this information includes the participants' sex, age, ethnicity, country of birth, country of residence, nationality, fluent languages, student status, and employment status.

Age and Sex. Figure 7 visualizes the distribution of the two pre-defined sex options, "Male" and "Female," across different age groups and attacks. Given existing OECD statistics (OECD, 2019), most of our participants are younger than the OECD median of 40. This bias towards younger demographics is common in online studies across different crowdsourcing platforms (see, e.g., (Stein et al., 2023)). All six experiments have a relatively balanced distribution between both sexes, though the female sex tends to be slightly overrepresented.

Student and Employment Status. As summarized in Tab. 7, full-time employees comprised the majority of participants across all six experiments, followed by part-time employees and unemployed citizens. The category "not in paid work" includes homemakers and retired or disabled citizens, while "starting soon" includes all participants who are due to start a new job within the next month (at the time of data collection). The trend towards fully employed participants also supports the skewness towards non-student participants, though Experiment 1 (SemAdv) has a particular bias towards non-student Prolific workers. The data expired flags for both statuses, which we also counted in Tab. 7, are set by Prolific.

Ethnicity. Figure 8 visualizes the participants' ethnicity for all six experiments. As we did not filter via Prolific's ethnicity prescreening, we (as of October 2024) only got access to a simplified ethnicity attribute where workers were asked to choose between general ethnicity categories (White, Black, Asian, Mixed, Other). While white citizens make up the majority of participants, the bias is not as strong as in

Status	SemAdv	cAdv	NCF	DA	AdvPP	ACA
(i) Student Status						
Yes	21	27	22	19	16	15
No	51	30	38	21	25	33
Data expired & Undefined	2	4	1	10	9	2
(ii) Employment Status						
Full-Time	41	30	27	30	28	28
Part-Time	8	11	15	5	6	11
Unemployed	11	9	8	2	3	5
Not in paid work	3	5	2	1	0	1
Other	5	3	6	3	3	3
Starting soon	2	0	1	0	0	0
Data expired & Undefined	4	3	2	9	10	2

Table 7 Overview of participants' student and employment status across all six experiments. The *data expired* flag is automatically set by Prolific.

related studies such as (Stein et al., 2023).

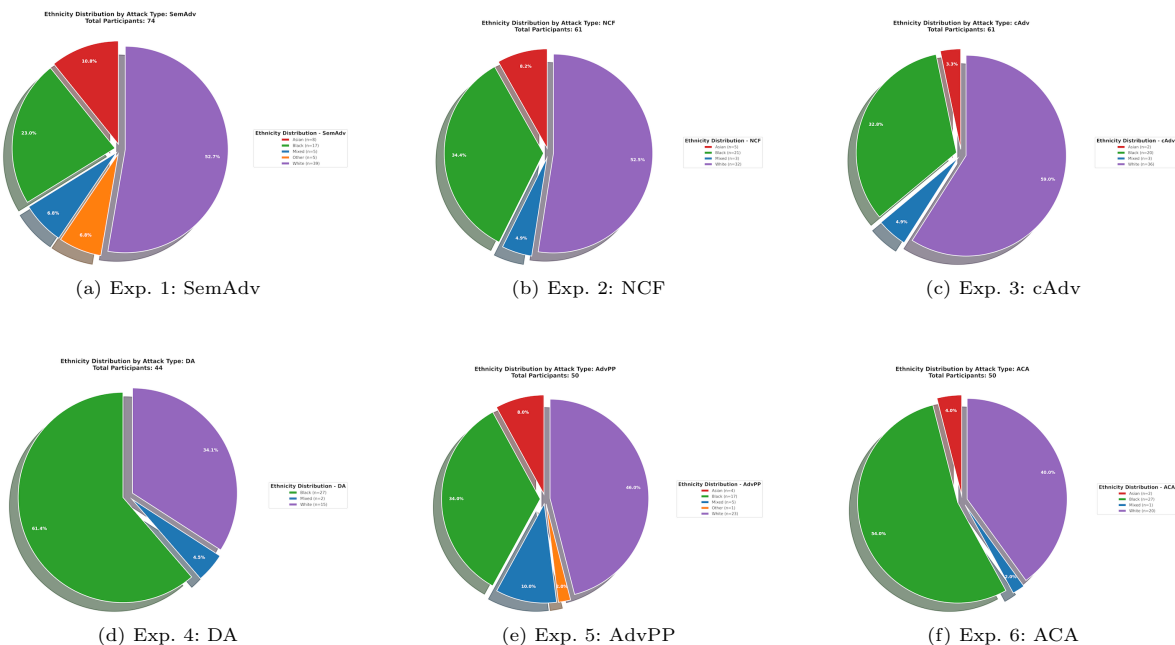


Fig. 8 Ethnicity distribution across all six experiments. The ethnicity labels provided by Prolific represent simplified categories of ethnicity.

Country of Residence. As part of this dissemination, we decided to summarize the attributes "country of residence," "country of birth," and "nationality" using the former demographic information, as there are no significant discrepancies between the three. As stated in Sec. 4.5, South African citizens are overrepresented in our experiment data. Additionally, citizens from Asian, American, and Oceanian countries are generally underrepresented. Compared to adjacent Prolific studies like (Stein et al., 2023),

the overrepresentation of South Africans is quite noticeable, whereas the underrepresentation of the latter three regions aligns with existing work. An exact breakdown of regions and countries of residence is depicted in Fig. 9.

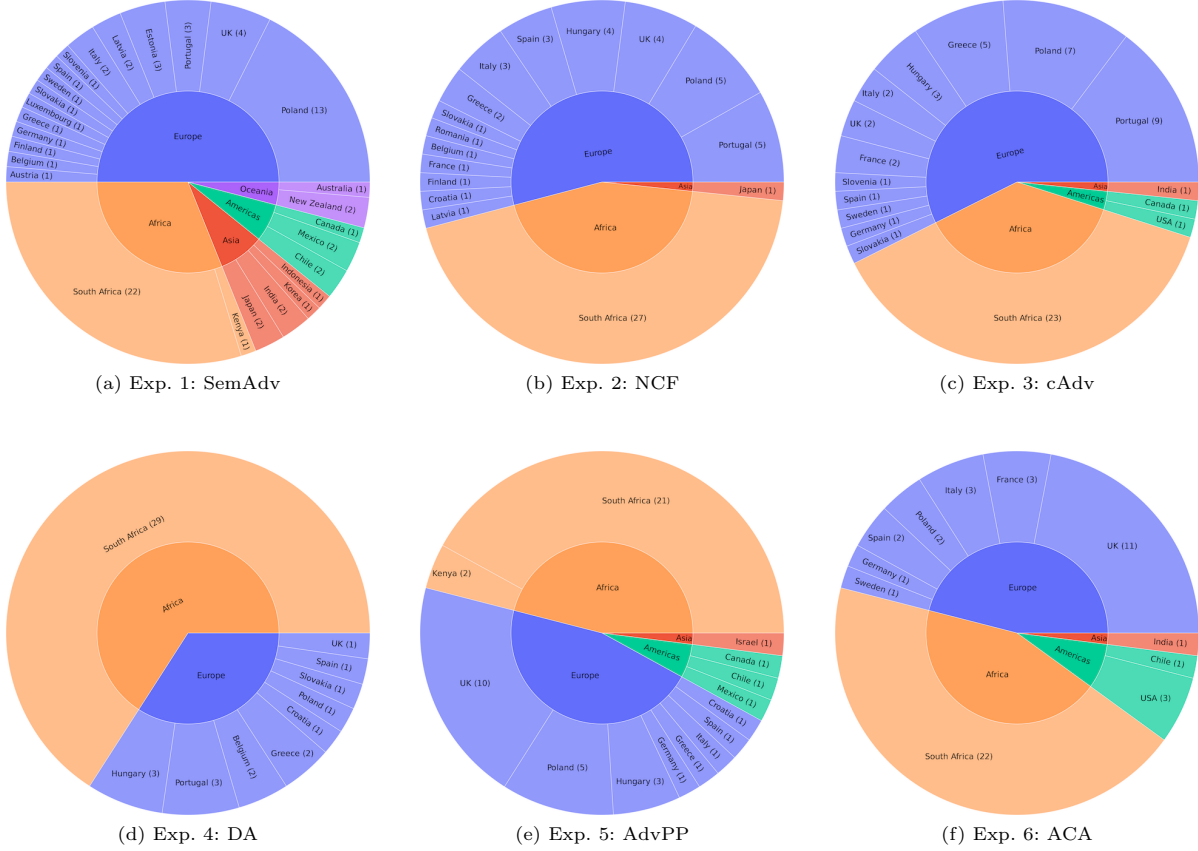


Fig. 9 Distribution of participants' country and region of residence across all six experiments. Note that Prolific participants almost exclusively reside in OECD countries.

Languages. Finally, we also have access to the self-reported fluent languages of participants, as visualized in Fig. 10. As expected and desired, the count of fluent English speakers equals the corresponding sample size. Furthermore, our participants predominantly speak Germanic, Romance, or Slavic languages. The underrepresentation of language families mainly spoken in Asia (e.g., Turkic or Sino-Tibetan languages) aligns with the previously observed lack of Asian citizens in our participant pool.

C.5 Cumulated Statistics across all Experiments

This subsection summarizes (i) the key performance metrics (Tab. 8) and (ii) the time statistics (Tab. 9) across all six experiments ($n = 346$). Additionally, we compared and assessed the observed relation between completion time and participants' performance (Fig. 11). Interestingly, we can observe that faster participants tend to perform better than slower workers. Due to a single wrongly tracked completion time, Tab. 9 and Fig. 11 only cover 345 instead of 346 participants.

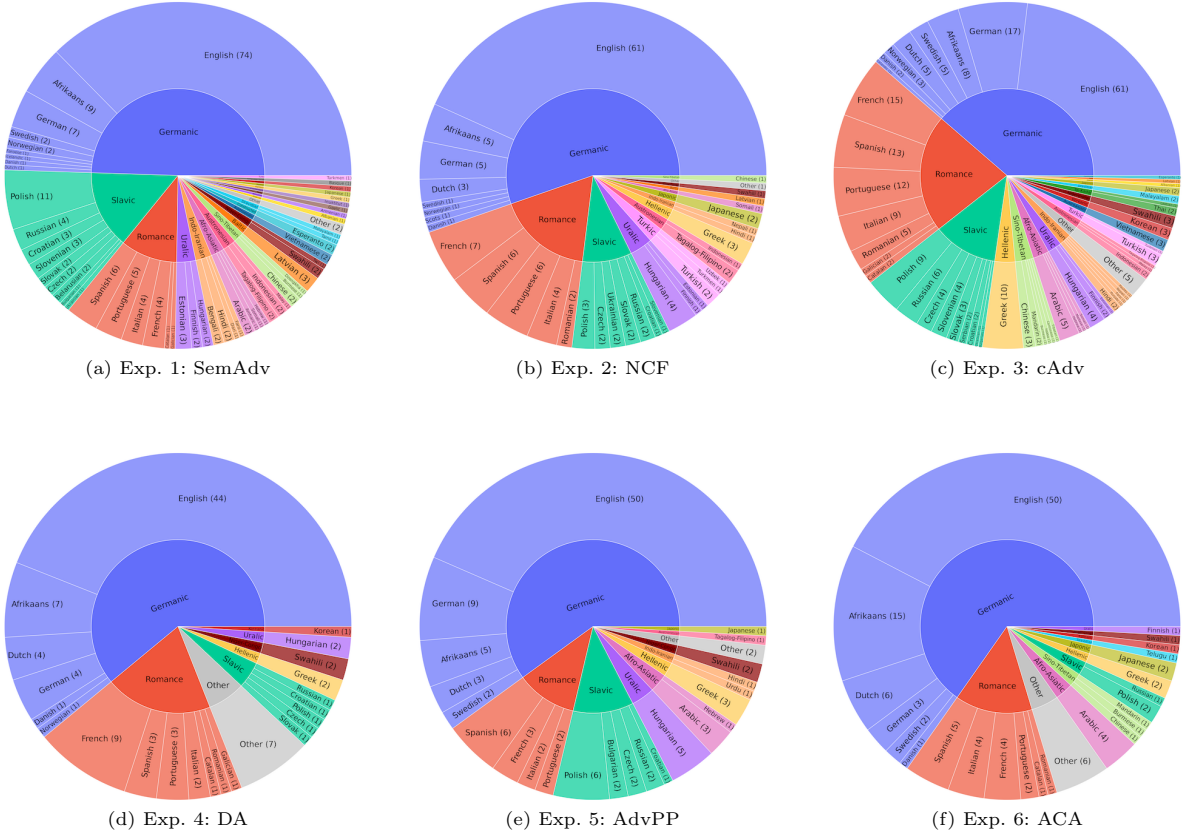


Fig. 10 Distribution of participants' self-reported fluent languages across all six experiments.

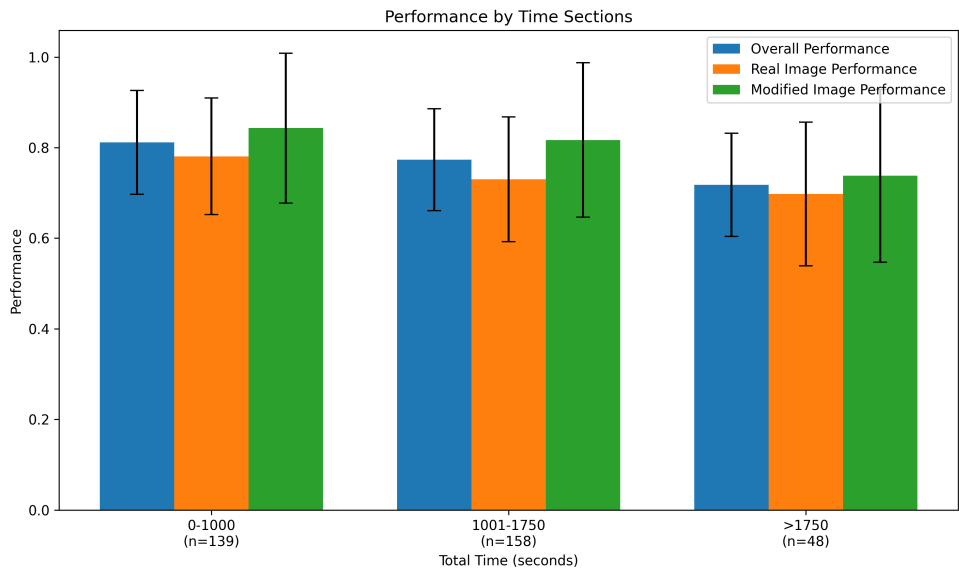


Fig. 11 Participants' performance on real and modified images in relation to their invested total time across all six experiments. We excluded one participant's time statistics due to technical errors (hence, $n = 345$).

ASR	μ_{Modified}	s_{Modified}	μ_{Real}	s_{Real}
0.3891	-1.262	1.171	0.8734	1.299

Table 8 Cumulated Key Performance Metrics of all six experiments ($n = 346$). We explain the metrics in Sec. 3.3.

(i) Total Time Needed (in minutes)					(ii) Time per Main Study Image (in seconds)				
Average	Std. Dev.	Median	Min.	Max.	Average	Std. Dev.	Median	Min.	Max.
19:51	08:48	18:08	05:29	52:21	6.807	3.252	6.018	1.989	21.053

Table 9 Cumulated time statistics ((i) total completion time and (ii) annotation time per image) across all six experiments. We excluded one participant’s time statistics due to technical errors (hence, $n = 345$).

C.6 System Prompt for GPT-4o-based Assessments

You are an expert image assessment assistant. Your task is to analyze images and rate them on a scale from -2 to +2:

- 2: Definitely modified (clear evidence of manipulation)
- 1: Probably modified (some signs of modification)
- 0: Unsure (cannot determine with confidence)
- +1: Probably real (appears unmodified but with some uncertainty)
- +2: Definitely real (clear evidence of being unmodified)

Follow these guidelines for assessment:

1. Real/Unmodified Images:

- Photographs captured using cameras or imaging devices
- Show scenes or objects as they naturally exist
- May have lower quality or unusual colors due to artificial lighting
- May appear less clear than modern images

2. Modified Images (consider these for negative ratings):

- Use of filters (Instagram, Snapchat, etc.)
- Partial or complete recoloring
- Addition or removal of objects
- Defective (“dead”) pixels or other pixel changes
- Unusual or unnatural coloring (e.g., greyscale)
- Non-color related modifications (e.g., unusually sharp edges)
- Minimal and subtle signs of modifications (inconsistent coloring, unusual lines)

3. Important Considerations:

- Some modifications are obvious, while others are subtle
- Real images may have lower quality due to being from early 2000s
- Indoor images may have unnatural colors due to artificial lighting
- If an image looks like it’s straight out of a camera without filters, it’s likely unmodified

Output ONLY the numerical rating (-2 to +2) with no additional text or explanation.

D Creating ImageNet S-R50-N

Distilling suitable images for the SCOOTER framework out of the initial 50,000 validation images involved several steps to ensure the quality and integrity of the dataset.

Step 1: Reassessed ImageNet Labels. Based on the reassessed labels of (Beyer et al., 2020), we filtered out all images that contained no ImageNet object (making them trivial AEs). Because the ImageNet classification models can only provide a single label per image, we also removed all images that display multiple ImageNet objects simultaneously (see Fig. 12 for some examples). After all, altering such images so that victim models classify them via one of the other legitimate labels would not represent actual adversarial examples. Applying this initial filter already left us with 39,394 images. Apart from the four ImageNet classes, *sunglass* (class id: 836), *notebook* (681), *sunglasses* (837), and *screen* (782), each class has at least five images.

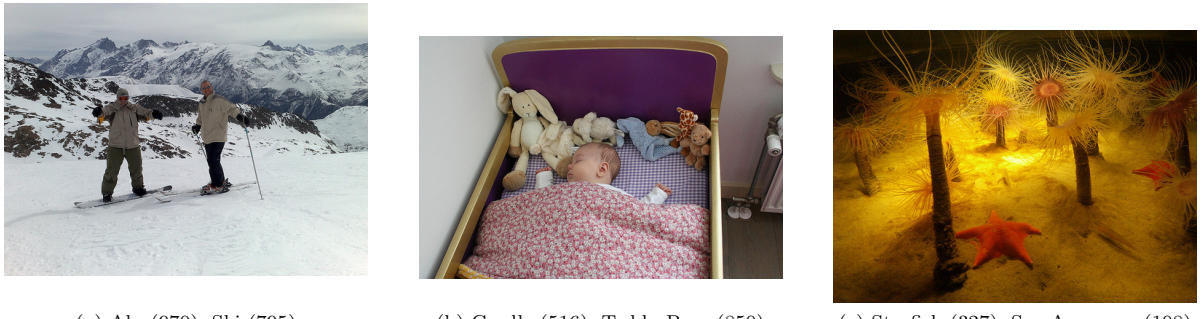


Fig. 12 Three ImageNet validation set images (Russakovsky et al., 2015) that display more than one ImageNet object according to Beyer et al. (2020). The caption of an image describes the depicted ImageNet objects and their label ID.

Step 2: The Initial Top-5 of ResNet-50-AT_{norm}. To further refine the dataset, we kept only images easily classified (i.e., correct high-confidence predictions) by our target model ResNet-50-AT_{norm} (Salman et al., 2020). We tried to collect the five easiest ImageNet instances of the 996 ImageNet classes that contain at least five images. However, for 12 classes, the model had fewer than five images, which it correctly classified. The resulting dataset, therefore, only contains 4,951 images.

Step 3: The Final and Clean Model-Specific Dataset. Based on the previous dataset, we now want to have a *clean* dataset. However, some images were inherently modified (e.g., via watermarks, copyrights, filters, discolorations, visible noise, or other artifacts), which we therefore removed. To ensure the dataset’s quality, the top five images of each class were manually inspected and filtered out if necessary. The goal was to retain *three usable* images per class. Where possible, the top three images were selected from the initial 4,951 images, attempting to salvage them through methods like cropping if they were otherwise usable. In cases where too many initial images were deemed unusable for a particular class, we supplemented the dataset with additional clean images that the target models correctly classified. The goal was to avoid any significant modifications.

Ultimately, our dataset should contain ca. 3,000 clean images. This refined dataset is the basis for generating adversarial examples (AEs). Only after this meticulous curation process would we generate AEs, ensuring that the experiments conducted on this dataset would build upon a solid, uncontaminated foundation. The final dataset associated with the robust model of (Salman et al., 2020) is our *ImageNet SCOOTER-ResNet50-Norm* (or simply ImageNet S-R50-N) dataset. We outline details about the dataset in the next section. Any changes made to the initial images of step 2 are also documented and will be made available online upon acceptance.

D.1 ImageNet S-R50-N Details

The final dataset comprises 2,966 images. During the refinement process, 109 images were added per step 3, affecting 73 classes. Of the original 1,000 classes, we marked 447 as "clean," meaning the top three easiest images for these classes contained no modifications and could be used without further adjustments. The following steps were taken for the remaining 553 classes:

- For 21 classes, the original top three images could be retained after minor cropping to remove small watermarks, making expanding the selection with top-five images unnecessary.
- For 73 classes, new images had to be introduced:
 - 55 of these classes were successfully expanded with additional clean images.
 - 1 class (websites) was entirely excluded, as these images are screenshots of web pages. However, this does not align with our provided definition of "real" images ("photographs captured using cameras or other imaging devices, showing scenes or objects as they naturally exist.").
 - For 17 classes, fewer than three valid images were available: 4 of these 17 classes had no relevant images, 6 had only one valid image, and 7 had exactly two valid images.

For the remaining 459 classes, the top three images had to be replaced with the top five selections, removing 626 images. Additionally, for 57 of these classes, some of the new top-five images required cropping to be usable. The reasons for the necessary replacements were varied, with multiple reasons often applying to a single class (see Fig. 13 for an overview of reasons). Reasons for replacements include not only different image modifications but also instances where the image is too small or depicts a virtual environment (e.g., a computer-rendered object).

D.2 Why not use the NIPS 2017 competition dataset?

In the previous two sections, we have established that ImageNet instances require significant pre-processing before researchers can use the images to assess unrestricted attacks. However, one could also resort to other existing ImageNet-like datasets, like the one used in the NIPS 2017 competition (Kurakin et al., 2018), which are predominantly used by the adversarial machine learning community. However, we decided against this dataset due to the following reasons:

1. It contains multiple images that are either modified (e.g., via watermarks) or may look modified to some humans (see Fig. 14 for some examples).
2. The victim model should easily correctly classify the real image baseline so that adversarial attackers would not get some AEs "for free."
3. Existing datasets tend to standardize the images' width and height, which is unrealistic. All ImageNet S-R50-N instances retain the original dimensions (excluding images we had to adjust per step 3 of our dataset creation process).

E Ablation Study: Gradual Inattentiveness Filtering

The hard rules of Tab. 1 act as strict reasons to filter out participants. While these metrics and the proposed additional 99th percentile filters are bound to filter outliers, it would be interesting to explore how softer, more gradual filters would influence the key performance metrics of SCOOTER. As such, we decided to analyze the impact of composite filter conditions, where participants will be flagged as inattentive after triggering *multiple* more lenient conditions. We focused on the color-based experiments (i.e., Experiments 1-3) only, as they are more similar to one another in terms of the time invested.

Soft and Hard Indicators of Inattentiveness. To define composite filters that take multiple more lenient conditions into account, we must first differentiate between strict (or hard) indicators and more lenient (or soft) filter conditions. Akin to our instant-out filters, we consider the respective percentiles of each metric based on our available data. Apart from the annotation time per image, all soft gradual

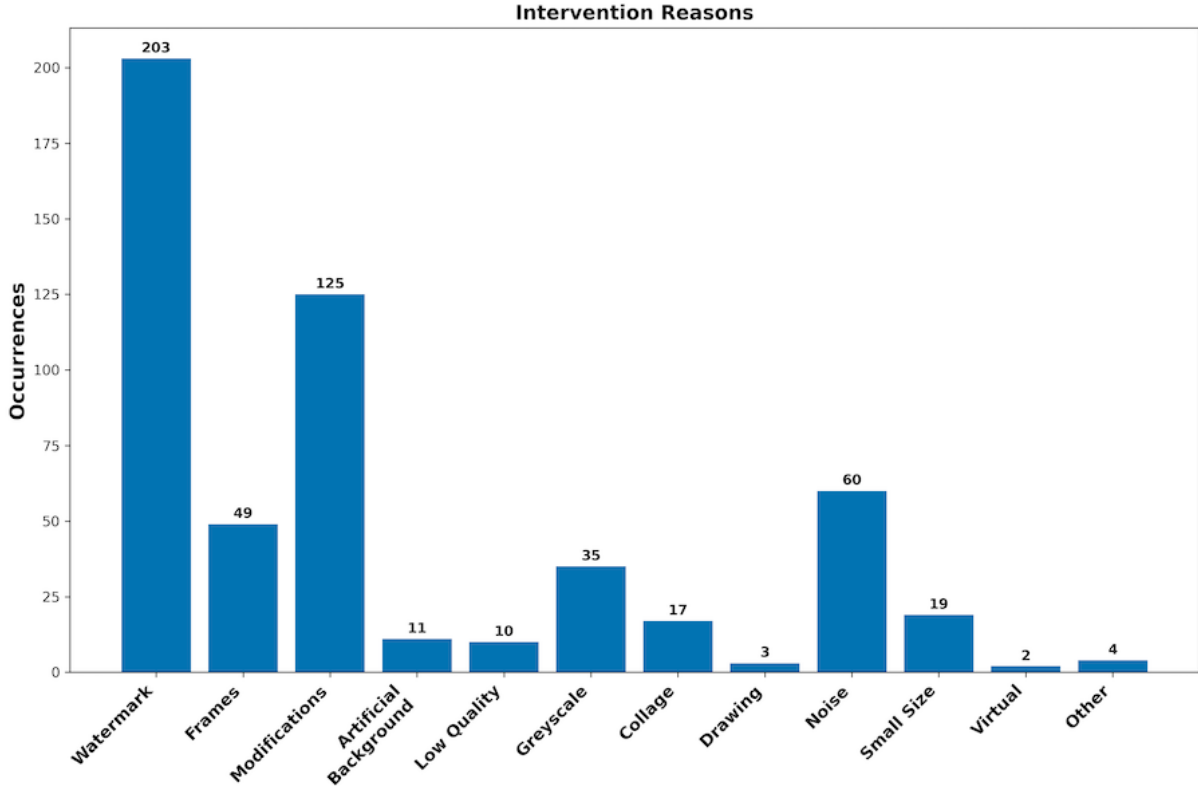


Fig. 13 Overview of intervention reasons within the refinement process (Step 3). The intervention on a single image can have more than one intervention reason. "Frames" includes images with colored borders, "modifications" includes images whose colors or edges were modified via, e.g., image filters, the "collage" category is reserved to image collages, and virtual images include computer-rendered objects and screenshots.

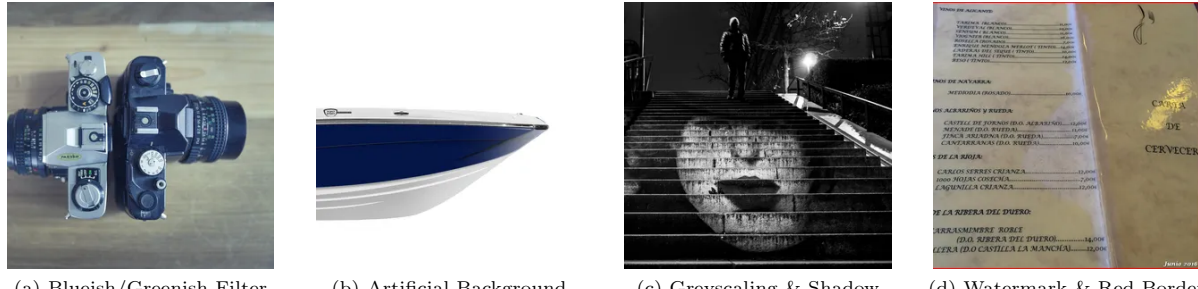


Fig. 14 Original NIPS 2017 competition (Kurakin et al., 2018) images that could look modified to participants. The caption of an image describes the reason(s) why annotators might rate them as *modified*.

conditions represent the 90th percentile of their metric, whereas hard gradual conditions represent 95th percentiles. We defined stricter thresholds for soft and hard annotation time indicators because faster participants tend to perform better on SCOOTER studies (see Fig. 11). Here, the soft threshold represents the 95th percentile, while the hard one represents the 99th percentile. Table 10 overviews soft and hard indicators for potential gradual composite filters. The overview excludes gradual thresholds for the median

sequence length, as 195/196 participants shared the median of two (hence, fine granular filtering is not feasible).

Metric	Soft Thresholds	Hard Thresholds
Average Time per Image	≤ 2.756 seconds	≤ 2.465 seconds
Max. Sequence Length	≥ 7	≥ 8
Mean Sequence Length	≥ 1.7168	≥ 1.8028
IRV _{real}	outside of [0.6818, 1.68006]	outside of [0.5923, 1.7505]
IRV _{modified}	outside of [0.106, 1.5517]	> 1.643

Table 10 Five soft and hard thresholds for granular composite filtering of inattentive participants.

E.1 The Effects of Gradual Inattentiveness Filtering

Figures 15 and 16 visualize the effects of gradual filtering on both the real and modified image ratings. The left heatmap of both figures visualizes the effect of filtering via n many hard and m many soft indicators. For instance, the value of row zero and column one (161) describes the number of participants that would remain if we were to filter out all participants who passed all instant-out filters ($n = 187$) but triggered *more than* zero hard and *more than* one soft threshold. Analogously, the remaining two heatmaps describe the effects of filtering on μ_{Real} and s_{Real} (Fig. 15) resp. μ_{Modified} and s_{Modified} (Fig. 16).

Both figures visualize general trends. For example, stricter filtering leaves us with participants who can better detect modified images (μ_{Modified} moves closer to -2) but who also struggle more with detecting real images (μ_{Real} moves away from $+2$). However, the discrepancies between the observed extrema are minuscule: across all possible hard-soft-filtering combinations, μ_{Modified} only changes by about 0.015 rating points, while μ_{Real} changes by ca. 0.04 rating points (see middle heatmap of Figs. 15 and 16). Similarly, the standard deviations s_{Real} and s_{Modified} remain consistent across all filtering combinations (see right heatmap of Figs. 15 and 16). Based on these findings, we currently cannot recommend using such additional filters.

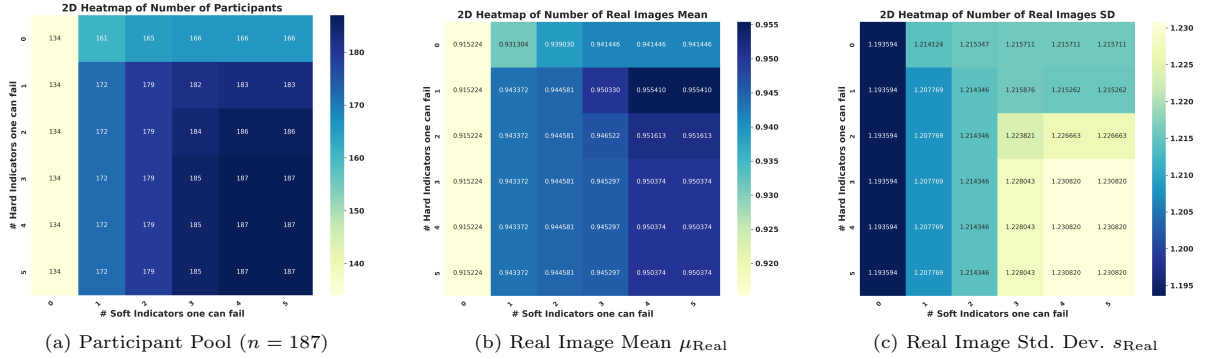


Fig. 15 The effects of gradual inattentiveness filtering on the existing participant pool (left; $n = 187$) and their respective real image rating statistics: μ_{Real} (center) and s_{Real} (right).

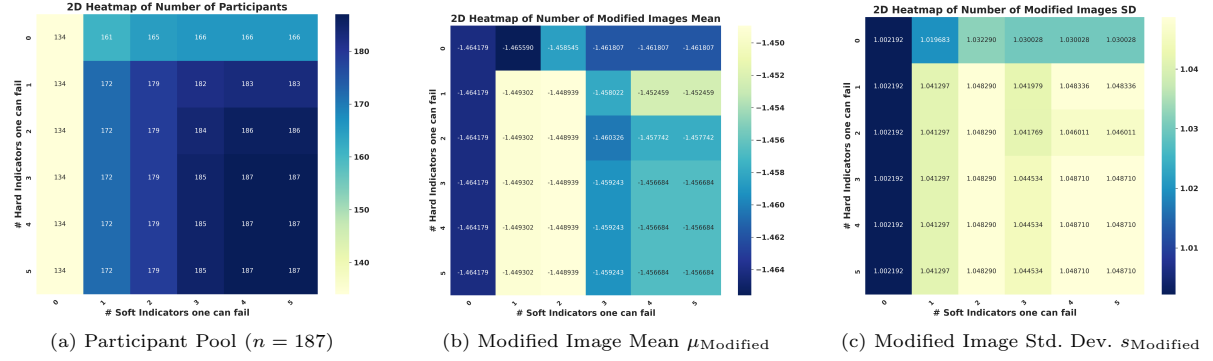


Fig. 16 The effects of gradual inattentiveness filtering on the existing participant pool (left; $n = 187$) and their respective modified image rating statistics: μ_{Modified} (center) and s_{Modified} (right).

F Ablation Study: The Effects of Simplifying the Comprehension Checks

As discussed in Sec. 4, a non-minuscule number of participants struggle to complete the comprehension check (failure rate: 12-14%). Consequently, we decided in Experiment 3 to let participants, who correctly answered only 4 of the 6 comprehension check pairs, attend the annotation phase. However, we did not include the annotations of the seven affected participants in our primary results of Sec. 5. Instead, we refer to Tab. 11 for a side-by-side comparison between the original results of Experiment 3 and those obtained when considering the additional seven samples. While the small sample size motivates further research into this problem, our initial findings indicate that a more lenient comprehension check does not significantly impact the final results of SCOOTER experiments. This also supports our earlier hypothesis in Sec. 4.5 that slight differences in the comprehension check procedures do not substantially affect participant comprehension, thanks to the consistent core screening criteria across experiments.

Metric	Original 5/6 threshold	More lenient 4/6 threshold
Sample Size	61	68
μ_{Modified}	-1.674	-1.6503
s_{Modified}	0.832	0.866
μ_{Real}	0.919	0.8902
s_{Real}	1.226	1.2406
$\Delta < \Delta_L$	1.899×10^{-40}	3.108×10^{-42}
$\Delta > \Delta_U$	1.000	1.000

Table 11 Comparison of key metrics between Experiment 3 participants who met the original comprehension check threshold (correctly classified at least 5 out of 6 pairs) and an expanded participant pool including the seven participants who correctly classified 4 out of 6 pairs.